CSIRO PUBLISHING

RESEARCH PAPER
https://doi.org/10.1071/WF23079

International Journal of WILDLAND FIRE
International Association of Wildland Fire

# GAMBUT field measurement of emissions from a tropical peatland fire experiment: from ignition to spread to suppression

Yuqi Hu[A,B], Thomas E. L. Smith[C], Muhammad A. Santoso[A,D], Hafiz M. F. Amin[A,E], Eirik Christensen[A], Wuquan Cui[A], Dwi M. J. Purnomo[A], Yulianto S. Nugroho[D] and Guillermo Rein[A,*]

For full list of author affiliations and declarations see end of paper

*Correspondence to:
Guillermo Rein
Department of Mechanical Engineering, Imperial College London, London, SW7 2AZ, UK
Email: g.rein@imperial.ac.uk

**Received:** 23 May 2023
**Accepted:** 5 August 2024
**Published:** 22 October 2024

**Cite this:** Hu Y *et al.* (2024) GAMBUT field measurement of emissions from a tropical peatland fire experiment: from ignition to spread to suppression. *International Journal of Wildland Fire* **33**, WF23079. doi:10.1071/WF23079



## ABSTRACT

**Background.** Accurate quantification of emissions from peatland wildfire is crucial for understanding their feedback to the atmospheric and Earth system. However, current knowledge on this topic is limited to a few laboratory and field studies, which report substantial variability in terms of the fire emission factors (EFs). **Aims.** We aim to understand how emissions vary across the life cycle of a peatland fire. **Methods.** In August/September 2018, we conducted the largest and longest to-date field-scale experimental burn on a tropical peatland in Sumatra, Indonesia. Field measurements of gas emissions from the fire experiment were conducted using an open-path Fourier transform infrared spectroscopy to retrieve mole fractions of 11 gas species. **Key results.** For the first time, we calculated and reported EFs from 40 measurement sessions conducted over 2 weeks of burning, encompassing different fire stages (e.g. ignition, smouldering spread, and suppression) and weather events (e.g. rainfall). Our findings provide field evidence to indicate that EFs vary significantly among fire stages and weather events. We also observed that the heterogeneous physicochemical properties of peatland site (e.g. moisture content) influenced the EFs. We also found that modified combustion efficiency was highly sensitive to complex field variables and could introduce large uncertainties when determining the regimes of a peat fire. **Conclusions and implications.** Further studies to investigate peat fire emissions are needed, and more comprehensive mapping of peatland heterogeneity and land use for emissions inventories, accounting for spatial and temporal variability in EFs since the initiation of a fire event is required.

**Keywords:** degraded peatland, emission factor, field measurement, fire emissions, fire spread, fire suppression, ignition, peat, weather effect.

## Introduction

Wildfire is an inherent component of the Earth system, resulting from natural processes. However, human interventions can alter the type and severity of the dominant ongoing ecological processes, and result in direct and indirect atmospheric feedbacks through emissions of gases and particulate matter (aerosols) (Bowman *et al.* 2009; Archibald *et al.* 2018). Among various types of wildfires, peatland fires, which are characterised by the largest fuel consumption on Earth (Rein 2013), play a significant role in contributing to greenhouse gas (GHG) emissions, particularly during dry periods (Turetsky *et al.* 2015; Hu *et al.* 2018*a*). For instance, it has been estimated that the Indonesian peatland fires associated with the 1997–1998 El Niño-Southern Oscillation (ENSO) event emitted approximately 0.8 to 2.6 Gt (1 Gt = $1 \times 10^9$ tonnes) of carbon, equivalent to 13–40% of the mean annual global carbon emissions from fossil fuels at that time (Page *et al.* 2002). Similarly, the 2015 Southeast Asian peat fire released approximately 1.5 Gt of net permanent $CO_2$ equivalent emissions into the atmosphere, resulting in the largest carbon emissions observed in the region since 1997 (Huijnen *et al.* 2016).

Peatland fires not only contribute to the global burden of GHGs, but also serve as a dominant source of primary and secondary organic aerosol emissions, leading to regional

air quality deterioration and visibility reduction in the form of haze events (Huang *et al.* 2014; Hu *et al.* 2018*a*; Plautz 2018; Wiggins *et al.* 2018). For instance, the 1997 Indonesian peat fire event caused transboundary haze across south-east Asia, impacting around 100 million people and resulting in estimated damages of USD4.5 billion (Heil and Goldammer 2001). In recent years, as global climate change has accelerated, peat fires have become more frequent and widespread, leading to increased exposure of the public to various pollutants, such as carbon monoxide (CO) and fine particles, present in haze (Kunii *et al.* 2002; Hu *et al.* 2018*a*; Plautz 2018). Epidemiological studies have shown that haze episodes during peatland fire events have resulted in increased mortality and morbidity, particularly affecting the respiratory and cardiovascular systems (Heil and Goldammer 2001; Shaposhnikov *et al.* 2014; Koplitz *et al.* 2016; Hu *et al.* 2018*a*). Currently, the haze crisis resulting from periodic peatland fires remains an unresolved environmental and health issue, particularly in south-east Asia, and has the potential to escalate into regional disputes and public criticism (Forsyth 2014).

Pristine tropical peatlands are typically characterised by a water-logged environment and high moisture content (Matysek *et al.* 2018), which naturally serve as a barrier against fires (Eggleston *et al.* 2006; Turetsky *et al.* 2015). However, factors such as natural droughts (e.g. El Niño) or human activities (e.g. anthropogenic drainage, deforestation, peat harvesting) can lower the moisture content of peat, making it susceptible to smouldering combustion, a slow, low temperature, and flameless burning process that is persistent in nature (Turetsky *et al.* 2015; Rein 2016).

Smouldering peat fires are characterised by a weak, white-grey smoke plume that accumulates close to the ground, which is different from the intense flaming forest fires (e.g. crown fires) with fast-moving diffusion flames and buoyant smoke plumes (Rein 2013; Hu *et al.* 2018*a*). These fires can be initiated by a weak ignition source in the natural environment and can sustain for weeks or even months (Rein 2013; Restuccia *et al.* 2017).

Slash-and-burn, a traditional farming method where natural vegetation is cut down and burned to clear land for cultivation, is commonly practiced in tropical peatlands prior to plantation activities (Cochrane 2003). A portion of the heat generated during surface fuel combustion is transferred to, and can ignite the thick layer of peat underground that can be up to 11 m deep, leading to uncontrolled and long-lasting smouldering peat fires (Usup *et al.* 2004; Page *et al.* 2011). These smouldering fires have a long residence time of heat, with peak temperatures typically ranging from 450 to 700°C, and can penetrate deeply into the ground, resulting in severe soil thermal damage, which can have lethal impacts on soil properties and local biological systems (Rein *et al.* 2008; Huang *et al.* 2016; Santoso *et al.* 2022). The extensive consumption of soil during peat fires not only involves the burning of ancient carbon (up to 10,000 years old), but also has the potential to cause long-term impacts on local vegetation, such as changes in flora species and incomplete vegetation recovery, in all types of peatland settings (Rein 2013; Kettridge *et al.* 2015; Hu *et al.* 2018*a*).

To comprehensively understand the feedback of fire emissions to the atmosphere and climate change, it is crucial to accurately quantify the emissions in atmospheric modelling (Eggleston *et al.* 2006; Akagi *et al.* 2011; Urbanski 2014). The emission factor (EF), which is defined as the mass of a species emitted per mass of dry fuel consumed (g $kg^{-1}$), is a fundamental input for estimating total emissions (Eggleston *et al.* 2006). Peat fire EFs obtained from two laboratory burns (Yokelson *et al.* 1997; Christian *et al.* 2003) were compiled and averaged in Akagi *et al.* (2011), providing support for atmospheric modelling communities such as the Global Fire Emissions Database (GFED) in calculating total fire emissions (van der Werf *et al.* 2017). However, in the document 'Supplement to the 2006 Guidelines for National Greenhouse Gas Inventories: Wetlands' published by the 2013 Intergovernmental Panel on Climate Change (IPCC), only EFs of $CO_2$–C, CO, and $CH_4$ at the IPCC Tier 1 (basic) level of methodological complexity were included. These EF values were adopted from only one study with a single laboratory burn of peat (Christian *et al.* 2003), which could introduce significant uncertainties in estimating global peat fire emissions and understanding their feedback (Hu *et al.* 2018*a*; Smith *et al.* 2018).

Field measurements that gather emission information from fires *in situ* provide valuable insights into fire and emission behaviour under natural conditions (Christensen *et al.* 2019). However, a review of peat fire EFs revealed that only a limited number of smoke emission measurements have been conducted in the field (Hu *et al.* 2018). Despite the scarcity of studies investigating peat fire emissions, there is considerable variability in EF values between studies, with some gas EFs varying by a factor of 10 (Akagi *et al.* 2011; Hu *et al.* 2018*a*).

Understanding the reasons behind this variability remains one of the biggest challenges in biomass burning emissions science (van Leeuwen and van der Werf 2011). On the one hand, peat fires are not stationary emission sources, as transient emissions are significantly influenced by combustion dynamics (Rein *et al.* 2009; Hu *et al.* 2018*b*). On the other hand, peatland conversion and management practices have been shown to affect fire EFs (Smith *et al.* 2018). Furthermore, natural variations in peat physicochemical properties, such as moisture content, inorganic content, and bulk density, have been demonstrated to have significant impacts on fire dynamics (Huang *et al.* 2016; Huang and Rein 2017; Hu *et al.* 2019, 2020; Cui 2022).

However, the roles of soil properties and meteorological conditions (for example, wind and rainfall) in influencing fire dynamics and emissions have not been thoroughly investigated in current field studies (Huijnen *et al.* 2016; Stockwell *et al.* 2016), which could hinder the development

of a higher-tier EF inventory at the intermediate Tier 2 or the most demanding Tier 3 level (Hiraishi *et al.* 2014). In this study, life-cycle emissions, which include emissions from ignition, spread, and suppression, were measured in a controlled tropical peatland fire experiment (GAMBUT, Indonesian word for 'peat') conducted in Sumatra, Indonesia. In addition to the emission measurements, this fire experiment considered and measured field-scale peat fire behaviour in terms of temperature, fire area, spread rate, and suppression, and these results have been reported in the twin paper of this study, in Santoso *et al.* (2022).

This work presents the findings of the emission measurements conducted during the GAMBUT fire experiment. Specifically, emissions from 40 fire smoke plumes belonging to four different fire categories observed in the field experiment (ember ignition, slash-and-burn, smouldering spread, and fire suppression) were measured using an open-path Fourier transform infrared (OP-FTIR) spectroscopy *in situ*. EFs of 11 gas species for Indonesian tropical peatland fires were reported, and field evidence was provided in this work to explain the inter-plume variability in EFs.

## Materials and methods

### Field site and peat soil characterisation

This controlled field-scale peatland fire experiment was conducted as part of the '1st GAMBUT Workshop: UK-Indonesia Collaboration for Mitigation of Peat Fires'. The objective of this workshop was to investigate the ignition, spread, emissions variability across the life cycle, and extinguishing of peatland fires. GAMBUT is the first study to fill the gap in the understanding of peat fire between laboratory and field scale, providing field evidence to formulate an effective and efficient mitigation response. The field fire experiment was specifically conducted from 19 August (Day 1) to 30 August (Day 12) 2018, in a secondary peat swamp area measuring 408 $m^2$ (34 m × 12 m) located in Rokan Hilir, Sumatra, Indonesia (Fig. 1). Climate history data suggests that the average temperature and humidity in the previous 5 years were 27.4 °C and 79.1%, and the mean daily rainfall in August is 6.5 mm, allowing for the investigation of peat fire emissions in a typical tropical environment (BMKG 2022; Santoso *et al.* 2022).

Site preparation was conducted prior to the ignition attempts. The peatland at the experimental site was manually divided into three separate and parallel plots, labelled as Plot 1, Plot 2, and Plot 3. There were live thick (>6 mm) fuels like palm trees, live thin fuels like ferns and sedges at the site. The original lush tropical plantation on each plot was manually cleared before the fire experiment. Specifically, dead thin fuel duff was kept intact for Plot 1, allowing the observation of its effect on slash-and-burn. Plot 2 and Plot 3 were left as bare peat ground with sparse palm tree roots (Fig. 2). Each plot had an interior dimension of 10 m × 10 m. Fire breaks, consisting of trenches 0.5 m wide

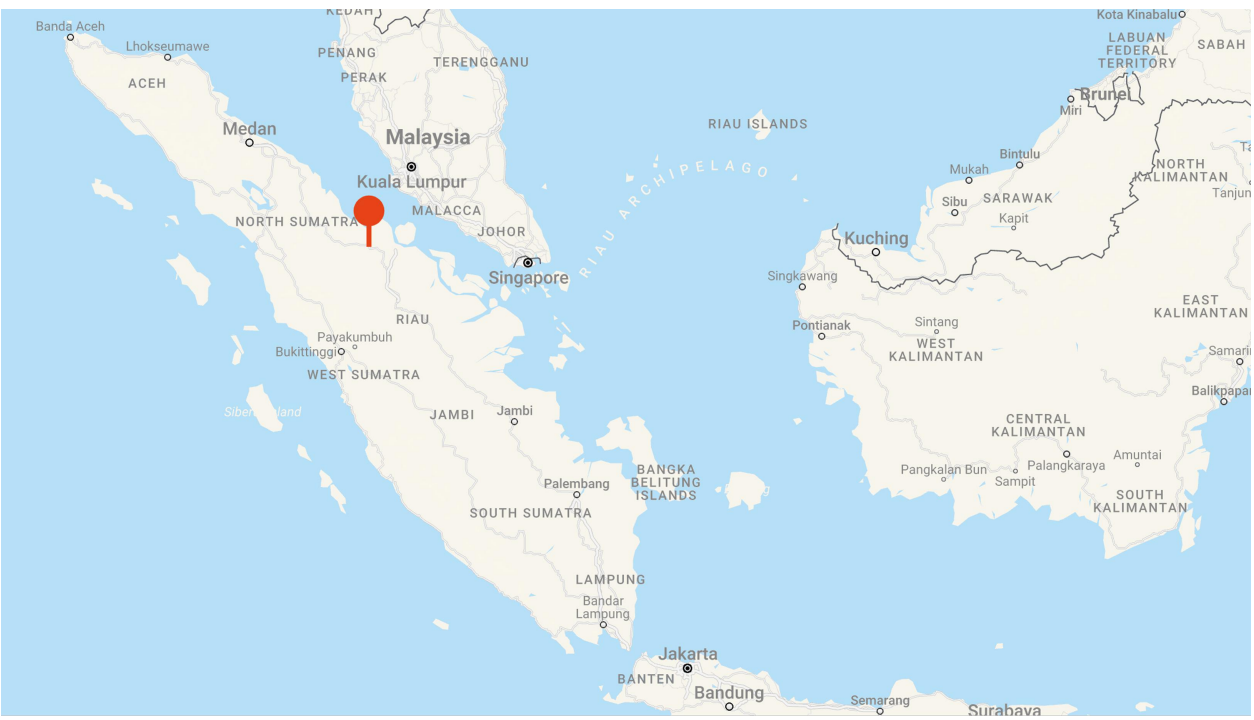


**Fig. 1.** Map of Sumatra and southern peninsula of Malaysia showing the location of the experimental site at Rokan Hilir, Sumatra, Indonesia (1°36′17.1″N, 100°58′30.5″E) (Map Data, Google, 2023).

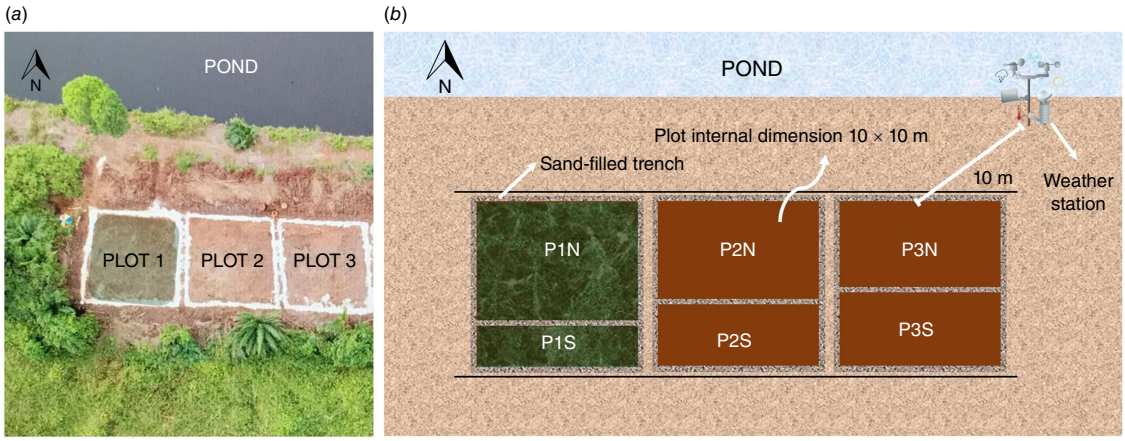


**Fig. 2.** Drone image showing the experimental site (a); Schematic of the experimental plots for GAMBUT peat fire experiment (b). Plot 1 was left with a shallow layer of surface litter vegetation thus was identified by green shading. The letters 'N' and 'S' in the plot name indicate the north and south sides of the plot, respectively.

and 0.5 m deep filled with sand, were constructed along the perimeter of each plot to prevent fires from spreading beyond the designated plot area.

Furthermore, each plot was divided into two sections: (1) the north side; and (2) the south side for different ignition and suppression attempts. Before the fire experiments, a thorough field site topology measurements were conducted, showing that there was an elevation difference of roughly 1 m between the north and south sides of the experimental site. A weather station was installed 10 m next to Plot 3 to monitor the atmospheric pressure, temperature, relative humidity, wind speed, and rain rate in the field. Further details about the experimental site in terms of the climate, topology, surface plantation, and surface treatment, are described in Santoso *et al.* (2022).

Representative peat sampling was conducted *in situ* prior to the ignition of the peatland to characterise the physico-chemical properties of the soil, including moisture content (dry basis), wet bulk density, inorganic content (dry basis), and elemental analysis (the content of C/H/N). The samples were weighed to obtain the wet bulk density. The moisture content in dry basis was calculated by using the volumetric moisture content (VMC) measured from a soil moisture sensor probe (Delta-T Devices Ltd, England) and the wet bulk density. The inorganic content of the peat samples was derived from burning the sample in a furnace at 1000°C. Detailed calculation and determination of the physico-chemical properties of the soil was elaborated in the twin paper of this study, in Santoso *et al.* (2022). This work follows the same metrics used in Santoso *et al.* (2022) in terms of the moisture and ash content in describing the soil properties, and in discussing the emission measurement results. For detailed locations of soil sampling, where PVC pipes were utilised to extract subterranean peat cores from nine sampling locations in each plot (0–40 cm depth), see Supplementary Fig. S1.

## Ignition methods and emission measurements

The experiment commenced with ignition attempts on Day 1 (19 August). A charcoal ember ignition method employed in Pastor *et al.* (2017), and the traditional slash-and-burn approach commonly used in the oil palm plantation industry for peatlands conversion into plantation sites (Cochrane 2003), were applied in this study to ignite the peat soil, and dead ferns and sedges in different locations of the experimental plots and at different dates, respectively (Table 1). Specifically, a total of 9.3 kg of charcoal was used to produce the embers that were put in three pits (each with dimensions of 0.5 m × 0.2 m and 0.2 m deep) at P1S on Day 1 and Day 3 (Santoso *et al.* 2022). The charcoals were firstly ignited with gasoline and left to burn for 10 min, and then put into the ignition pit. Slash-and-burn, involving piling and igniting dry dead plantation materials such as tree branches, leaves, and litter, with dimensions of 8 m length × 1 m width × 0.5 m height, was conducted at P1N, P2N, and P3N on Day 5 and Day 7, respectively (Fig. 3). Details regarding the charcoal and slash-and-burn ignition protocols are provided in the twin paper of this study, in Santoso *et al.* (2022).

Self-sustained smouldering was determined by visual observation of ground fire spread and fire size, and by examining the temperature profile of the soil using thermocouple readings and infra-red (IR) signatures (see Santoso *et al.* (2022) for details). Following successful ignition, the peatland started to smoulder from Day 2, slowly spreading towards unburned peatland areas and releasing fire smoke into the ambient air throughout the experiment.

**Table 1.** Summary of the 40 *in situ* peat fire emission measurements in 2018.

| Measurement number[A] | Field event[B] | Date | Day in the field | Measurement start time | Measurement end time | Atmospheric pressure (mb) | Temperature (°C) | Humidity (%) | Wind speed (m s$^{-1}$) | Rain rate (mm h$^{-1}$) | Location | Path length (m) |
|---|---|---|---|---|---|---|---|---|---|---|---|---|
| EI1 | Ember ignition | 19 August | 1 | 13:16 hours | 14:47 hours | 1008.8 | 33.1–34.5 | 51–60 | 1.5–2.3 | 0 | P1S | 10.5 |
| EI2 | Ember ignition | 19 August | 1 | 17:26 hours | 17:36 hours | 1006.8 | 33.7–33.9 | 54–56 | 1.28 | 0 | P1S | 10.5 |
| EI3 | Ember ignition | 19 August | 1 | 17:58 hours | 18:29 hours | 1006.5 | 32.4–33.5 | 54–60 | 1.08–1.59 | 0 | P1S | 10.5 |
| SS1 | Smouldering spread | 20 August | 2 | 11:13 hours | 12:13 hours | 1008.2 | 30.1–31.2 | 68–72 | 1.59–1.8 | 0 | P1S | 10.5 |
| SS2 | Smouldering spread | 20 August | 2 | 12:53 hours | 13:04 hours | 1007.5 | 32.2–32.4 | 62–65 | 2.3–2.4 | 0 | P1S | 10.5 |
| SS3 | Smouldering spread | 20 August | 2 | 14:34 hours | 15:46 hours | 1007.1 | 32.9–34.0 | 52–60 | 1.38–2.1 | 0 | P1S | 10.5 |
| SS4 | Smouldering spread | 20 August | 2 | 17:16 hours | 18:18 hours | 1005.6 | 31.2–31.8 | 64–76 | 0.8–1.4 | 0 | P1S | 10.5 |
| SS5 | Smouldering spread | 21 August | 3 | 10:14 hours | 10:47 hours | 1009.0 | 28.7–30.8 | 69–78 | 0.8–1.8 | 0 | P1S | 10.0 |
| EI4 | Ember ignition | 21 August | 3 | 12:06 hours | 12:17 hours | 1006.5 | 32.9–33.2 | 59–61 | 2.1–2.7 | 0 | P1S | 10.0 |
| EI5 | Ember ignition | 21 August | 3 | 13:29 hours | 14:35 hours | 1005.8 | 33.1–34.8 | 52–60 | 1.3–2.1 | 0 | P1S | 10.0 |
| EI6 | Ember ignition | 21 August | 3 | 16:39 hours | 17:40 hours | 1004.3 | 30.4–31.8 | 68–80 | 0–0.6 | 0 | P1S | 10.0 |
| SS6 | Smouldering spread | 22 August | 4 | 09:58 hours | 10:28 hours | 1009.4 | 28.7–29.5 | 69–72 | 1.8 | 0 | P1S | 10.5 |
| SS7 | Smouldering spread | 22 August | 4 | 10:39 hours | 11:14 hours | 1009.2 | 29.6–30.3 | 63–70 | 1.3–1.9 | 0 | P1S | 10.5 |
| SS8 | Smouldering spread | 22 August | 4 | 11:27 hours | 13:23 hours | 1008.6 | 31.2–32.1 | 57–60 | 1.9–2.3 | 0 | P1S | 10.5 |
| SS9 | Smouldering spread | 22 August | 4 | 16:19 hours | 17:51 hours | 1005.3 | 30.1–31.0 | 60–63 | 1.3–2.4 | 0 | P1S | 10.5 |
| SS10 | Smouldering spread[C] | 22 August | 4 | 18:20 hours | 18:52 hours | 1006.3 | 27.6–29.3 | 70–81 | 0.8–1.3 | 0 | P1S | 10.5 |
| SS11 | Smouldering spread[D] | 23 August | 5 | 10:51 hours | 11:11 hours | 1010.6 | 31.5–32.2 | 50–55 | 1.9–2.8 | 0 | P1S | 11.0 |
| SS12 | Smouldering spread[E] | 23 August | 5 | 11:26 hours | 12:29 hours | 1009.5 | 32.2–32.9 | 49–53 | 2.1–2.9 | 0 | P1S | 11.0 |
| SB1 | Slash-and-burn | 23 August | 5 | 13:23 hours | 13:35 hours | 1008.0 | 33.3–33.5 | 48–51 | 2.4–2.6 | 0 | P1N | 15.5 |
| SS13 | Smouldering spread | 23 August | 5 | 13:37 hours | 14:23 hours | 1007.4 | 33.3–34.2 | 45–51 | 1.9–2.6 | 0 | P1N | 16.0 |
| SS14 | Smouldering spread | 23 August | 5 | 15:59 hours | 16:33 hours | 1006.1 | 33.8–34.1 | 46–50 | 1.6–2.1 | 0 | P1N | 16.0 |
| SS15 | Smouldering spread | 23 August | 5 | 17:28 hours | 17:59 hours | 1006.0 | 32.9–33.7 | 49–53 | 0.8–1.3 | 0 | P1S | 17.0 |
| SB2 | Slash-and-burn | 23 August | 5 | 18:11 hours | 18:30 hours | 1006.3 | 32.1–32.7 | 53–63 | 0–0.6 | 0 | P3N | 12.0 |
| SB3 | Slash-and-burn[F] | 23 August | 5 | 18:35 hours | 19:08 hours | 1006.6 | 29.9–31.9 | 55–71 | 0–0.6 | 0 | P3N | 10.0 |
| SS16 | Smouldering spread | 24 August | 6 | 11:57 hours | 12:27 hours | 1008.8 | 33.0–34.2 | 44–51 | 1.4–1.8 | 0 | P1N | 11.5 |
| SS17 | Smouldering spread | 24 August | 6 | 13:14 hours | 13:46 hours | 1007.7 | 33.4–33.8 | 47–50 | 1.4–2.1 | 0 | P1S | 11.5 |

(*Continued on next page*)

**Table 1.** (*Continued*)

| Measurement number[A] | Field event[B] | Date | Day in the field | Measurement start time | Measurement end time | Atmospheric pressure (mb) | Temperature (°C) | Humidity (%) | Wind speed (m s$^{-1}$) | Rain rate (mm h$^{-1}$) | Location | Path length (m) |
|---|---|---|---|---|---|---|---|---|---|---|---|---|
| SS18 | Smouldering spread | 24 August | 6 | 16:09 hours | 16:41 hours | 1005.8 | 32.2–32.7 | 51–54 | 1.6–2.3 | 0 | P1S | 10.5 |
| SS19 | Smouldering spread[G] | 24 August | 6 | 19:48 hours | 19:58 hours | 1009.0 | 23.6–23.7 | 92–93 | 0.8–1.1 | 5.6 | P1N | 11.0 |
| SS20 | Smouldering spread | 25 August | 7 | 10:55 hours | 11:34 hours | 1009.5 | 29.4–30.8 | 64–69 | 0.8–1.4 | 0 | P1S | 11.0 |
| SS21 | Smouldering spread | 25 August | 7 | 12:39 hours | 13:11 hours | 1008.6 | 32.1–32.3 | 57–62 | 1.3–1.4 | 0 | P1N | 11.0 |
| SB4 | Slash-and-burn | 25 August | 7 | 13:35 hours | 14:06 hours | 1007.3 | 32.2–33.1 | 54–59 | 1.1–1.4 | 0 | P2N | 10.0 |
| SS22 | Smouldering spread | 26 August | 8 | 10:06 hours | 11:43 hours | 1008.8 | 29.9–32.6 | 58–71 | 1.4–2.3 | 0 | P1N | 12.0 |
| SS23 | Smouldering spread | 26 August | 8 | 17:46 hours | 18:47 hours | 1004.1 | 32.3–35.0 | 40–60 | 0–1.3 | 0 | P1N | 12.0 |
| SS24 | Smouldering spread | 27 August | 9 | 09:57 hours | 11:00 hours | 1010.2 | 30.5–31.8 | 59–64 | 0.9–1.4 | 0 | P1N | 12.0 |
| SS25 | Smouldering spread | 27 August | 9 | 11:25 hours | 12:26 hours | 1009.1 | 31.7–33.1 | 49–60 | 1.4–1.8 | 0 | P2N | 10.5 |
| SS26 | Smouldering spread | 27 August | 9 | 17:39 hours | 18:21 hours | 1005.5 | 31.9–32.4 | 59–65 | 0.8–0.9 | 0 | P1N | 12.0 |
| SS27 | Smouldering spread | 29 August | 11 | 10:11 hours | 11:52 hours | 1010.8 | 26.9–31.2 | 61–79 | 0.8–1.4 | 0 | P1N | 11.0 |
| SP1 | Suppression | 29 August | 11 | 13:14 hours | 13:33 hours | 1008.6 | 32.8–33.3 | 54–60 | 1.1–1.3 | 0 | P2N | 13.0 |
| SP2 | Suppression | 29 August | 11 | 15:47 hours | 17:00 hours | 1006.3 | 31.7–33.6 | 54–61 | 1.3–1.8 | 0 | P1S | 11.5 |
| SP3 | Suppression | 29 August | 11 | 17:39 hours | 18:40 hours | 1005.8 | 30.7–31.2 | 66–69 | 1.3–2.1 | 0 | P1N | 13.5 |

[A]EI, ember ignition; SS, smouldering spread; SB, slash-and-burn; SP, suppression.
[B]This column displays the observed fire category in the field.
[C]A short shower happened before the measurement.
[D]A metal sheet was used to cover an overhang formed in the process of smouldering spread at P1S.
[E]The metal sheet was removed prior to the measurement.
[F]Smoke plumes stems from residual vegetation smouldering fire were mixed with smoke plume from slash-and-burn.
[G]Peak transient rain rate was recorded as 32.3 mm h$^{-1}$.

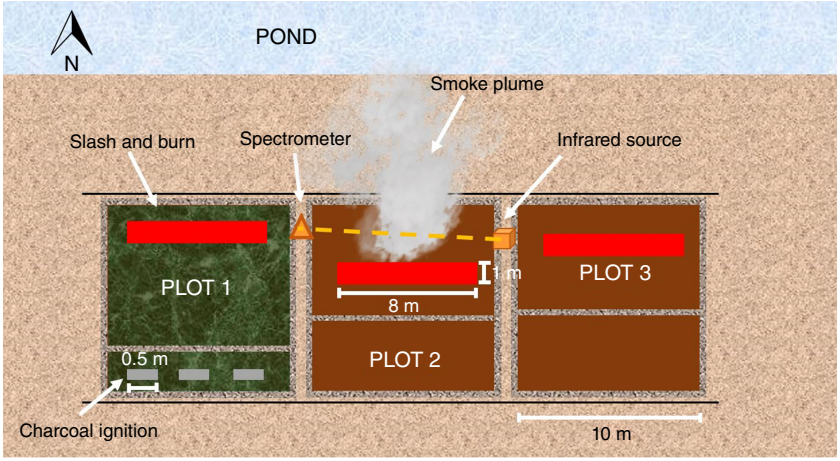


**Fig. 3.** Schematic of locations of ember and slash-and-burn ignition attempts and an example of fire smoke plume measurement using a Fourier-transform infrared spectroscopy in the field.

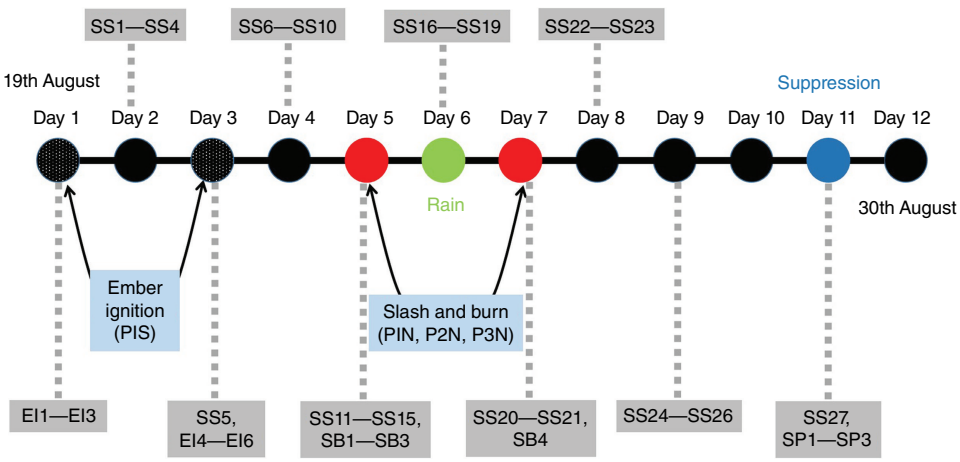


**Fig. 4.** Timeline of the GAMBUT fire emission measurements from ignition to suppression. A total of 40 fire smoke plume measurements were conducted. Measurements from four fire types and stages, ember ignition (EI), smouldering spread (SS), slash-and-burn (SB), and suppression (SP) were included in this sketch.

Fig. 4 shows the timeline of the fire emission measurements from ignition to suppression. Specifically, a metal sheet was used in this study to cover a burning spot on Day 5 (23 August) when smouldering spread steadily, attempting to investigate the influence of limited oxygen supply on the emissions from the smouldering spread (Rein 2016). On Day 6, natural rainfall event occurred, with rain rate reaching an average of 5.6 mm $h^{-1}$ for more than 10 min. On Day 11 and Day 12, a water spray and a direct injection device were used to suppress and terminate the fires. Details regarding the suppression devices and protocols are illustrated in Santoso *et al.* (2022). In this work, a total of 40 different smoke plume measurement periods were undertaken for the characterisation of the life-cycle emissions including four fire type and stages observed in the field: ember ignition (EI), slash-and-burn (SB), smouldering spread (SS), and fire suppression (SP). In total, there were six ember ignition (EI1–EI6), 27 smouldering spread (SS1–SS27), four slash-and-burn (SB1–SB4), and three suppression (SP1–SP3) fire smoke measurements.

Gas emissions from the fire smoke plumes were measured by using an open-path Fourier transform infrared spectroscopy (OP-FTIR). The OP-FTIR collects the real time spectra that contained absorption features for 13 target gases ($CO_2$, CO, $CH_4$, $NH_3$, acetylene ($C_2H_2$), ethylene ($C_2H_4$), ethane ($C_2H_6$), methanol ($CH_3OH$), formaldehyde ($CH_2O$), formic acid (HCOOH), hydrogen cyanide (HCN), acetic acid ($CH_3COOH$), and nitrous oxide ($N_2O$)). The OP-FTIR system used in this study consisted of a MIDAC Corporation M2000 Series FTIR spectrometer equipped with a Stirling-cooled mercury-cadmium-telluride detector and fitted with a MIDAC custom-built 76 mm Newtonian telescope. The spectrometer was mounted on an adjustable tripod to provide stable support for signal reception from a remotely located infrared source, which consisted of a 12-V silicon carbide glowbar operating at 1500 K fitted in front of a 20-cm diameter gold-plated collimator (Smith *et al.* 2018). The use of the OP-FTIR system for collecting biomass burning gas spectra has been detailed in previous studies (Wooster *et al.* 2011; Paton-Walsh *et al.* 2014; Smith *et al.* 2014).

In total, more than 9000 gas spectra were collected from these measurements. A forward modelling method combining the use of the Multiple Atmospheric Layer Transmission (MALT) program (Griffith 1996) and absorption line


**Fig. 5.** Photographs showing a typical set-up of OP-FTIR measuring emissions from ember ignition (*a*, EI4), slash-and-burn (*b*, SB1), smouldering spread (*c*, SS23), and water spray suppression (*d*, SP3).

parameters adopted from the 2016 HITRAN transmission molecular absorption database (Gordon *et al.* 2017) were used to derive the path-averaged trace gas mole fractions. The spectral regions of the trace gases that contain the most sensitive features from (Paton-Walsh *et al.* 2014) were selected and fitted with synthetic spectra from MALT to retrieve the gas mole fractions for a known path length and meteorological parameters (atmospheric pressure and temperature) (Paton-Walsh *et al.* 2014; Smith *et al.* 2014, 2018). The derived gas mole fractions from the forward modelling method are expressed in μmol mol$^{-1}$ (ppm) and were found to have trustworthy accuracy (within 5%) and a small uncertainty of 3–5% for $CO_2$, CO, and $CH_4$ (Smith *et al.* 2011; Stockwell *et al.* 2016).

Fig. 5 shows four typical field emission measurements conducted during ember ignition, slash-and-burn, smouldering spread, and suppression attempts using the OP-FTIR. Each measurement period lasted between 10 and 110 min. Given the relatively short time slots for each plume measurement period (<2 h), compared with the broader scope of the fire evolution process (>2 weeks), each measurement period was deemed to be within a relatively steady fire stage (Hu *et al.* 2018*b*). Table 1 summarises the general information of the 40 peat fire smoke plume measurements.

## Emission factor and combustion efficiency quantification

Generally, there are two methods for calculating the EF of gaseous species from peat fires: (1) the mass loss approach; and (2) the carbon balance approach. The mass loss approach is mainly used in small-scale laboratory experiments where the mass loss rate of the peat is measured for calculating EF (Eqn 1) (Rein *et al.* 2009; Hu *et al.* 2018*b*):

$$\mathrm{EF}_i = \frac{\dot{m}_i''}{\dot{m}''} \tag{1}$$

where $\dot{m}_i''$ is the mass flux of the released species $i$ (g s$^{-1}$ m$^{-2}$), and $\dot{m}''$ is the mass loss rate (fuel consumption rate) of the dry peat (g s$^{-1}$ m$^{-2}$).

The carbon balance approach is widely used in the literature to characterise peat fire emissions in the field

(Stockwell *et al.* 2014, 2016; Smith *et al.* 2018). The carbon balance approach does not measure the mass loss of the peat, which is impractical in field measurements. instead, it requires information of the fuel carbon content. This approach assumes all carbon-containing emissions are measured (Eqn 2) (Ward and Radke 1993):

$$\mathrm{EF}_i = F_\mathrm{c} \times 1000\,(\mathrm{g\,kg^{-1}}) \times \frac{MWi}{12} \times \frac{C_i}{C_\mathrm{T}} \quad (2)$$

wwhere $F_\mathrm{c}$ is the carbon content of the fuel (%), $\mathrm{MW}_i$ is the molecular weight of species $i$ (g mol$^{-1}$); 12 is the atomic mass of carbon (g mol$^{-1}$), $C_i$ is the number of moles of species $i$ (mol), and $C_\mathrm{T}$ is the total number of moles of carbon emitted (mol).

Both approaches have been verified in a laboratory-scale peat fire emission study (Hu *et al.* 2019). In this study, the carbon balance approach was used to derive the EFs of 11 targeted trace gas species. Ash-corrected carbon content of peat from the sampling locations across our site (Fig. S1) was calculated using Eqn 3:

$$F_{\mathrm{c-corrected}} = \frac{F_\mathrm{s}}{1 - \mathrm{IC}} \quad (3)$$

where $F_{\mathrm{c\text{-}corrected}}$ is the ash-corrected carbon content of the fuel (%), $F_\mathrm{s}$ is the carbon content of the soil sample obtained from the elemental analysis (%), IC is the inorganic (ash) content of the soil sample in dry basis (%). For a summary on the carbon content, inorganic content, and ash-corrected carbon content of the fuel burnt across the experimental site, see Table S1.

In Eqn 2, the determination of $C_i/C_\mathrm{T}$ can be either calculated directly from the measured excess mole fractions from the OP-FTIR (Eqn 4) or using emission ratio (ER) with respect to a reference species (Eqn 5) (Paton-Walsh *et al.* 2014):

$$\frac{C_i}{C_\mathrm{T}} = \frac{\Delta(i)}{\Sigma_{j=1}^{n}(\mathrm{NC}_j \times \Delta(j))} \quad (4)$$

where $\Delta(i)$ and $\Delta(j)$ are the excess mole fractions of species $i$ and $j$, respectively. The excess mole fraction is defined as the mole fraction measured (i) minus the mole fraction from the background $(i)_\mathrm{background}$, $\mathrm{NC}_j$ is the number of carbon atoms in species $j$, and the sum is of all carbon-containing species emitted by the fire:

$$\frac{C_i}{C_\mathrm{T}} = \frac{\mathrm{ER}_{i/\mathrm{CO}}}{\Sigma_{j=1}^{n}(\mathrm{NC}_j \times \mathrm{ER}_{j/\mathrm{CO}})} \quad (5)$$

where $\mathrm{ER}_{i/\mathrm{CO}}$ is the ER of species $i$ to the reference species (CO in this work) (Eqn 6) (Smith *et al.* 2018):

$$\mathrm{ER}_{i/\mathrm{CO}} = \frac{[i] - (i)_\mathrm{backgroud}}{[\mathrm{CO}] - (\mathrm{CO})_\mathrm{backgroud}} \quad (6)$$

When the amount of data used for regression is abundant, deriving the ER from the gradient of the linear best fit between species $i$ and CO does not necessarily entail the knowledge of background mole fractions, yet introduces very low uncertainty (Wooster *et al.* 2011). Given the large amount (9000+) of spectra collected in this study and the negligible mole fraction of trace gases in the background, an 'emission ratio to reference gas' method (Paton-Walsh *et al.* 2014) was used to derive the EF for a particular species (except $CO_2$ and CO) (Eqn 7):

$$\mathrm{EF}_i = \mathrm{ER}_{i/\mathrm{CO}} \times \frac{\mathrm{MW}_i}{\mathrm{MW}_\mathrm{CO}} \times \mathrm{EF}_\mathrm{CO} \quad (7)$$

where $\mathrm{MW}_i$ is the molecular weight of species $i$ (g mol$^{-1}$), $\mathrm{MW}_\mathrm{CO}$ (28.01 g mol$^{-1}$) is the molecular weights of CO, and $\mathrm{EF}_\mathrm{CO}$ is the EF of CO (g kg$^{-1}$).

In this work, $\mathrm{EF}_\mathrm{CO}$ and $\mathrm{EF}_{\mathrm{CO}_2}$ are calculated by using a 'summation method' (Eqs. 8, 9) (Paton-Walsh *et al.* 2014; Smith *et al.* 2018). This method has a significant advantage providing accurate EF values but requires accurate background information to calculate the total excess amounts of each gas species (Paton-Walsh *et al.* 2014). As a result, background spectra collection using the OP-FTIR was carried out prior to each smoke plume measurement, ensuring a good knowledge of the mole fractions of trace gas species from the background.

$$\mathrm{EF}_\mathrm{CO} = F_{\mathrm{c-corrected}} \times 1000\,(\mathrm{g\ kg^{-1}}) \times \frac{28.01}{12} \times \frac{\Delta\mathrm{CO}}{\Sigma_{j=1}^{n}(NC_j \times \Delta j)} \quad (8)$$

$$\mathrm{EF}_{\mathrm{CO}_2} = F_{\mathrm{c-corrected}} \times 1000\,(\mathrm{g\,kg^{-1}}) \times \frac{44.01}{12} \times \frac{\Delta\mathrm{CO}_2}{\Sigma_{j=1}^{n}(\mathrm{NC}_j \times \Delta j)} \quad (9)$$

where $\Delta\mathrm{CO}_2$ and $\Delta\mathrm{CO}$ are the summed excess mole fractions of $CO_2$ and CO, respectively. $\Delta j$ is the summed excess mole fractions of all carbon-containing species measured in this work ($CO_2$, CO, $CH_4$, $C_2H_4$, $C_2H_6$, $CH_3OH$, $CH_3COOH$, $CH_2O$, and HCN). These species account for ~>98% of all carbon emissions, omission of further carbonaceous species has been estimated to inflate the EFs by 1–2% (Yokelson *et al.* 2007).

In this work, modified combustion efficiency (MCE) from the four fire categories (ember ignition slash-and-burn, smouldering spread, and suppression) observed during the experiment was compared and discussed. MCE is defined as a proxy indicating the completeness of a combustion process (Ward and Hao 1991). The calculation of MCE is built on the use of the excess mole fractions of $CO_2$ ($\Delta[CO_2]$) and CO ($\Delta[\mathrm{CO}]$) (Eqn 10) (Ward and Radke 1993; Yokelson *et al.* 1996). MCE has been used as a universal standard in the literature to determine the importance of flaming or

smouldering in a fire (Christian *et al.* 2003; Stockwell *et al.* 2014; Urbanski 2014; Wilson *et al.* 2015):

$$\mathrm{MCE} = \frac{\Delta[CO_2]}{\Delta[CO_2] + \Delta[CO]} \quad (10)$$

## Results

### Peat soil properties

Table 2 provides the properties including density, moisture content, inorganic content and the content of C/H/N of the peat soil sampled among the four plots (P1N, P1S, P2N, P3N) where the emission measurement campaign were carried out. Detailed physicochemical properties of the whole peatland site across depths investigated were shown in the twin paper of this work in Santoso *et al.* (2022). Significant variability was observed in terms of the physicochemical properties across the peatland site, P1S showed a lowest mean moisture content of 53.5 ± 18.7%, while P2N exhibited the highest mean moisture content (264.9 ± 136.2%) across depths measured. Wet bulk density ranged from 656 to 1483 kg $m^{-3}$, with P1S (773.5 ± 79.6 kg $m^{-3}$) and P1N (1326.8 ± 147.8 kg $m^{-3}$) presenting the smallest and largest mean bulk density, respectively. In contrast, P1S and P1N exhibited the largest and smallest mean inorganic content across depths, respectively.

Elemental analysis result showed that P1S has the lowest mean carbon content (23.93%), while the largest peat carbon content value (31.3%) comes from P2N. In general, peat sampled from the experimental site has a lower carbon content than typical tropical peat (~55–60%) and a higher inorganic content compared with tropical peatland of 3 ± 1.96%, thus is deemed as degraded peat (Santoso *et al.* 2022). This degraded peat soil is commonly found in regions where the palm tree plantation industry is prevalent (Jauhiainen *et al.* 2016), which normally had undergone anthropogenic interference, such as drainage, logging, and agricultural conversion, as reported in previous studies (Page *et al.* 2011; Turetsky *et al.* 2015).

### Gas mole fractions and emission ratio

Fig. 6 shows an example of transient path-averaged mole fractions of $CO_2$ and CO from a slash-and-burn attempt (SB3). It is evident that $CO_2$ and CO, two species predominantly generated from char oxidation (Rein *et al.* 2009), followed a similar evolution pattern. Owing to wind and natural convective processes in the field, there was significant variance in the gas mole fractions determined from the OP-FTIR throughout the measurements, with peak concentrations of $CO_2$ and CO reaching approximately 1100 and 200 ppm, respectively.

To minimise the mixture of the adjacent smoke plumes, the path-averaged mole fractions of each measured gas species were retrieved from the OP-FTIR that was positioned directly above the actively burning peat. Furthermore, background mole fractions containing any possible emissions from the other adjacent burns were measured and

**Table 2.** Depth-averaged peat properties from the *in situ* measurement of the experimental plots.

| Measurement locations | Wet bulk density (kg $m^{-3}$) | Moisture content (%, dry mass basis) | Inorganic content (%, dry mass basis) | Elemental analysis | | |
|---|---|---|---|---|---|---|
| | | | | C (%) | H (%) | N (%) |
| P1N | 1326.8 | 173.9 | 34.2 | 30.14 | 9.9 | 0.78 |
| P1S | 773.5 | 53.5 | 58.7 | 23.9 | 2.34 | 1.21 |
| P2N | 1121.8 | 264.9 | 43.9 | 31.3 | 5.6 | 1.3 |
| P3N | 1143.8 | 151.2 | 52.4 | 26.1 | 4.79 | 1.09 |

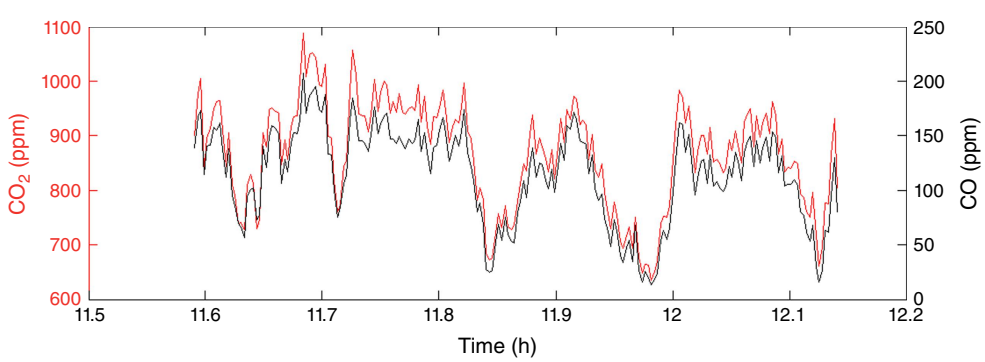


**Fig. 6.** Example time series of path-averaged mole fractions $CO_2$ and CO from a slash-and-burn smoke plume (SB3).

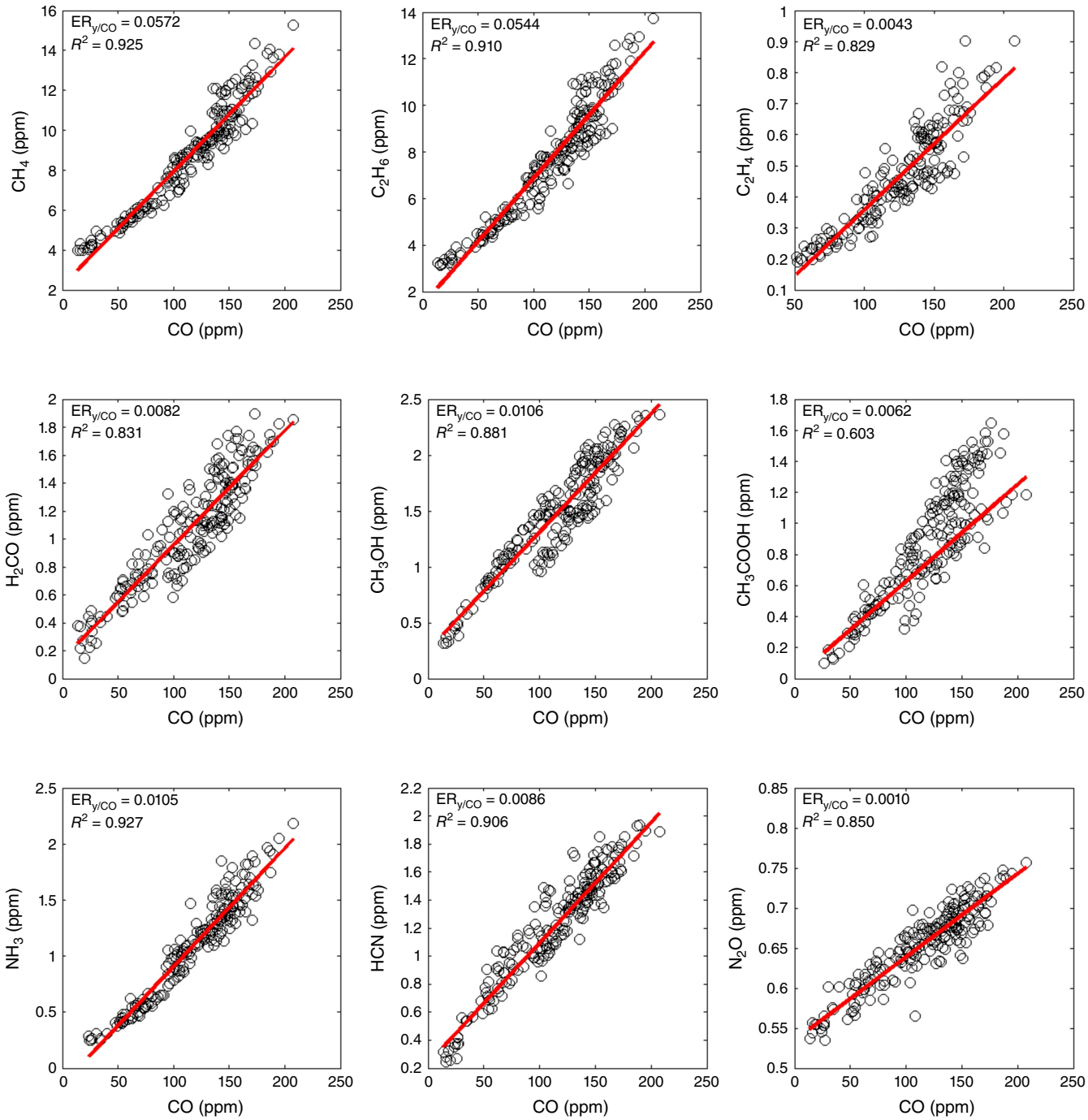


**Fig. 7.** Example emission ratios ($ER_{i/CO}$) and the $R^2$ value of the measured gases in SB3, calculated from gradient of the linear best fit between y species ($CH_4$, $C_2H_4$, $C_2H_6$, $H_2CO$, $CH_3OH$, $CH_3COOH$, $NH_3$, HCN, and $N_2O$) and CO.

subtracted from the calculated results. It is worth noting that some smoke plume measurements conducted during ember ignition and suppression exhibited gaps in the time series of gas mole fractions (e.g. EI2 and SS26, see Fig. S2), possibly attributable to periods of low signal-to-noise within the spectral window used for the retrieval of $CO_2$ and CO (Smith *et al.* 2018).

Fig. 7 shows a series of ER plots for investigated gas species against CO, for smoke plume SB3. Most species have a good correlation between species and excess mole fractions, indicating a well-mixed smoke plume in the field (Stockwell *et al.* 2016; Smith *et al.* 2018). Table S2 summaries ER values for investigated species against CO for all smoke plume measurements.

### Emission factors and inter-plume emission factor variability

Summing up the excess mole fractions of all measured carbon-containing species, the EFs of $CO_2$ and CO were calculated using Eqns 8 and 9. Combining the EF of CO and the ER of the targeted species against CO, the EFs of the remaining nine gas species were calculated using Eqn 7. Table 3 summarises the EFs and the associated uncertainty of analysed gas species for all 40 fire smoke measurements (Paton-Walsh *et al.* 2014; Smith *et al.* 2018). In addition to the 11 species reported in this work, we attempted to retrieve $C_2H_2$ and HCOOH but these were either below the detection limit of the OP-FTIR, or had a very poor emission ratio correlation with CO ($R^2 < 0.2$); thus, these are not included.

Fig. 8 shows the individual EFs for $CO_2$, CO, $CH_4$ and $NH_3$, the four prominent peat fire gas species that are important for greenhouse gas accounting and air quality modelling. The figure shows the inter-plume variability across 40 smoke plume measurements. $CO_2$ exhibits large EF variability throughout the experiment. The percentage difference, defined as the difference between two values divided by the average of the two values expressed as a percentage (Smith *et al.* 2018), reached 90% between EI1 and SS26 where the maximum (2540.0 ± 254 g $kg^{-1}$) and the minimum (962.0 ± 96.2 g $kg^{-1}$) values of the $CO_2$ EF were derived, respectively. Substantial inter-plume variability in terms of the EF percentage difference was found for CO (154%), $CH_4$ (165%) and $NH_3$ (170%) throughout the experiment. The maximum EFs of CO (412.7 ± 41.2 g $kg^{-1}$), $CH_4$ (10.5 ± 1.4 g $kg^{-1}$) and $NH_3$ (8.5 ± 0.3 g $kg^{-1}$) were from smouldering spread smoke plumes, while the minimum EFs of those species were mostly obtained from slash-and-burn smoke plumes characterised by stoichiometric and complete flaming combustion (Rein 2016).

## Discussion

### EF variability among fire/fuel types and fire stages

Fig. 9 compares the classified EFs of all detected species from four fire events (ember ignition, slash-and-burn, smouldering spread and suppression) observed in the field. Table 4 summarises the mean EFs of the smoke plumes from each fire category, and study-averaged EFs for all gas species measured. In general, gas emissions differ significantly among fuel types and fire categories (Rein 2016; Hu *et al.* 2019). Comparatively, ember ignition (EI1–EI6) has the largest $CO_2$ EFs (2446.5 ± 67.8 g $kg^{-1}$), averaging 56% higher than those from slash-and-burn, smouldering spread and suppression. This is mainly because the value of $CO_2$ EF is proportional to the carbon content of the fuel (Eqn 8). The charcoal ember consumed within this fire event has distinctively higher carbon content (78%) than those from peat (51.3–57.8%) and surface vegetation (55.0%) (Table S1), thus leading to a much higher EF value of $CO_2$. This finding verifies the important role of fuel composition affecting fire emissions (Yokelson *et al.* 1996; Akagi *et al.* 2011; Smith *et al.* 2018; Hu *et al.* 2018*a*).

The surface vegetation burnt from slash-and-burn (SB1–SB4) and peat burnt from smouldering spread peat (SS1–SS27) have similar carbon content. In comparison, slash-and-burn has 6% higher $CO_2$ EF (1693.4 ± 98.4 g $kg^{-1}$) but ~40 and ~66% lower CO EF (127 ± 73.3 g $kg^{-1}$) and HCN EF (1.2 ± 0.46 g $kg^{-1}$) than those from smouldering spread. This is attributed to the fact that slash-and-burn is dominated by flaming combustion, which has a higher combustion efficiency and a higher conversion ratio of the carbon from the fuel to complete combustion products (e.g. $CO_2$) than smouldering (Rein 2016; Hu *et al.* 2018*a*). The EFs of $CH_3OH$ (1.67 ± 0.95 g $kg^{-1}$), $CH_2O$ (3.2 ± 1.2 g $kg^{-1}$), and $CH_3COOH$ (5.2 ± 5.4 g $kg^{-1}$) from slash-and-burn stayed close to their corresponding EF values from the burning of crop residue reported in Akagi *et al.* (2011). In this field measurement, smouldering spread showed a ~300% times higher EF value (3.57 ± 2.03 g $kg^{-1}$) than flaming slash-and-burn for $NH_3$, a typical incomplete combustion product and a critical nitrogenous species for forming haze (Plautz 2018). This agrees with the findings from the literature that EFs of $NH_3$ from smouldering peat were significantly higher than flaming biomass burning (Akagi *et al.* 2011; Hu *et al.* 2019).

Plume-averaged EFs of $CO_2$ (1591 ± 243 g $kg^{-1}$), CO (206.4 ± 85 g $kg^{-1}$), $CH_2O$ (1.2 ± 0.5 g $kg^{-1}$), $CH_3OH$ (2.08 ± 1.24 g $kg^{-1}$), $CH_3COOH$ (4.7 ± 2.0 g $kg^{-1}$), $NH_3$ (3.57 ± 2.03 g $kg^{-1}$), and HCN (3.4 ± 1.7 g $kg^{-1}$) from smouldering spread at this degraded peatland stayed within the range of their EFs reported in the literature (Huijnen *et al.* 2016; Stockwell *et al.* 2016; Smith *et al.* 2018). EFs $CH_4$ (4.3 ± 2.4 g $kg^{-1}$) and $C_2H_4$ (0.4 ± 0.16 g $kg^{-1}$) measured during smouldering spread stayed at the low end of those reported in peer studies, while the EF of $C_2H_6$ (5.6 ± 2.6 g $kg^{-1}$) stayed at the high end (Hu *et al.* 2018*a*). The inclusion of these new EFs in the EF inventory could contribute to a better understanding of emissions and their inherent variability for degraded tropical peatland fires.

Gas emissions from suppression attempts (SP1–SP3) were investigated for the first time in this experiment. Significant variability was found for EFs for most species. For example, the EF for CO from the suppression stage stayed between 68.5 and 391.4 g $kg^{-1}$, while $CH_4$ and $NH_3$ EFs ranged between 2.9–9.3 and 1.0–8.3 g $kg^{-1}$, respectively. The large variability of the EFs seen at this fire stage is possibly caused by the limited amount of smoke plume measured ($n = 3$) at different peatland locations (P1N, P1S, P2N) as well as the different methods (water spray and injection) and water usage used in each fire suppression attempt (Santoso *et al.* 2022), likely affecting combustion efficiency and emissions in different ways.

**Table 3.** Emission factors (g kg $^{-1}$, dry basis) for all 40 fire smoke plume measurements.[A]

| Smoke plume #[B] | $CO_2$ | CO | $CH_4$ | $C_2H_4$ | $C_2H_6$ | $CH_2O$ | $CH_3OH$ | $CH_3COOH$ | $NH_3$ | HCN | $N_2O$ |
|---|---|---|---|---|---|---|---|---|---|---|---|
| EI1 | 2540.4 (254.1) | 201.9 (20.1) | – | – | – | – | – | – | – | – | 4.7 (2.2) |
| EI2 | 2422.7 (242.2) | 243.8 (24.3) | 2.3 (1.6) | – | – | – | – | – | – | – | 3.2 (2.0) |
| EI3 | 2512.9 (251.2) | 196.5 (19.6) | 3.3 (1.2) | – | – | – | – | – | 2.2 (0.1) | 1.1 (0.1) | 1.8 (1.2) |
| SS1 | 1846.9 (184.6) | 150.0 (15.0) | 1.6 (1.1) | – | – | – | – | – | 1.4 (0.1) | 1.7 (0.2) | 1.0 (0.6) |
| SS2 | 1635.2 (163.5) | 269.2 (26.9) | 3.6 (1.9) | – | – | – | – | – | 8.5 (0.3) | 4.6 (0.3) | 0.8 (0.6) |
| SS3 | 1712.0 (171.2) | 191.7 (19.1) | 2.0 (3.4) | – | – | – | – | – | 2.9 (0.2) | 2.9 (0.6) | 1.1 (0.3) |
| SS4 | 1598.2 (159.8) | 260.0 (26.0) | 3.2 (3.3) | – | – | – | 2.2 (0.4) | – | 4.3 (0.4) | 5.1 (0.7) | 0.9 (0.2) |
| SS5 | 1959.3 (195.9) | 86.7 (8.6) | 2.9 (0.6) | – | – | – | 0.8 (0.1) | – | 1.1 (0.1) | 0.9 (0.1) | 0.5 (0.3) |
| EI4 | 2372.0 (237.2) | 208.4 (20.8) | 10.0 (1.5) | 1.5 (0.1) | 9.9 (1.9) | 1.7 (0.2) | 2.2 (0.2) | – | 4.0 (0.4) | 5.4 (0.5) | 2.1 (0.3) |
| EI5 | 2471.8 (247.1) | 208.5 (20.8) | 2.8 (1.8) | – | – | – | 1.2 (0.1) | – | 2.8 (0.2) | 2.3 (0.3) | 1.5 (0.3) |
| EI6 | 2359.3 (235.9) | 225.8 (22.5) | 4.5 (1.2) | 0.3 (0.1) | 11.6 (1.9) | – | 1.9 (0.1) | – | 3.2 (0.3) | 3.2 (0.4) | 1.4 (0.1) |
| SS6 | 1997.2 (199.7) | 58.2 (5.8) | 1.1 (0.9) | – | – | – | – | – | 1.0 (0.1) | 0.9 (0.1) | – |
| SS7 | 1952.0 (195.2) | 85.7 (8.5) | 1.0 (0.9) | – | – | – | 0.7 (0.1) | – | 1.0 (0.1) | 1.2 (0.1) | – |
| SS8 | 1937.3 (193.7) | 93.3 (9.3) | 1.5 (1.0) | – | – | – | – | – | 1.8 (0.1) | 1.7 (0.2) | – |
| SS9 | 1777.0 (177.7) | 139 (13.9) | 3.7 (0.9) | – | 1.9 (1.8) | – | 1.0 (0.1) | – | 1.9 (0.1) | 2.0 (0.3) | 0.6 (0.3) |
| SS10 | 1767.1 (176.7) | 156.3 (15.6) | 2.8 (0.8) | – | 2.7 (1.6) | 0.7 (0.1) | – | – | 1.6 (0.1) | 1.5 (0.1) | 0.7 (0.2) |
| SS11 | 1631.4 (163.1) | 170.2 (17) | 5.4 (1.3) | – | 6.8 (3.6) | – | – | – | 2.4 (0.2) | 2.3 (0.1) | 0.7 (0.4) |
| SS12 | 1272.7 (127.2) | 330.5 (33) | 9.5 (1.5) | – | 9.8 (5.3) | – | 2.0 (0.5) | 6.4 (0.7) | 5.8 (0.5) | 6.5 (0.4) | – |
| SB1 | 1751.3 (175.1) | 54.1 (5.4) | 2.2 (1.1) | 0.8 (0.2) | 2.0 (2.5) | 1.4 (0.3) | 0.5 (0.1) | 1.0 (0.1) | 0.7 (0.1) | 0.5 (0.1) | 0.3 (0.2) |
| SS13 | 1461.1 (146.1) | 239.8 (23.9) | 7.4 (0.8) | 1.1 (0.1) | – | 2.3 (0.2) | 3.5 (0.3) | 5.6 (0.3) | 3.4 (0.2) | 2.4 (0.2) | 1.0 (0.1) |
| SS14 | 1461.4 (146.1) | 214.7 (21.4) | 4.7 (2.2) | – | – | – | – | 0.5 (0.1) | 2.5 (0.2) | 3.7 (0.6) | 0.9 (0.8) |
| SS15 | 1609.6 (160.9) | 253.3 (25.3) | 4.2 (0.9) | 0.7 (0.1) | 4.5 (1.2) | 1.7 (0.1) | 3.6 (0.5) | 5.8 (0.3) | 3.1 (0.2) | 5.0 (0.5) | 0.3 (0.2) |
| SB2 | 1780.7 (178.0) | 88.3 (8.8) | 4.0 (0.8) | 3.7 (0.1) | 4.2 (1.2) | 4.6 (0.1) | 1.1 (0.1) | 2.1 (0.2) | 0.8 (0.1) | 0.8 (0.1) | 0.2 (0.1) |

(*Continued on next page*)

**Table 3.** (*Continued*)

| Smoke plume #[B] | $CO_2$ | CO | $CH_4$ | $C_2H_4$ | $C_2H_6$ | $CH_2O$ | $CH_3OH$ | $CH_3COOH$ | $NH_3$ | HCN | $N_2O$ |
|---|---|---|---|---|---|---|---|---|---|---|---|
| SB3 | 1528.0 (152.8) | 247.8 (24.7) | 8. 1 (0.8) | 1.8 (0.1) | 8.6 (1.0) | 3.7 (0.2) | 3.0 (0.3) | 3.3 (0.3) | 1.5 (0.1) | 2.0 (0.2) | 0.4 (0.1) |
| SS16 | 1445.4 (144.5) | 197.3 (19.7) | 3.4 (0.7) | – | 4.3 (1.9) | – | 2.1 (0.1) | – | 3.8 (0.3) | 4.1 (0.3) | 0.7 (0.2) |
| SS17 | 1513.9 (151.3) | 264.3 (26.4) | 5.9 (1.1) | – | 6.7 (3.0) | – | 2.7 (0.3) | – | 4.4 (0.4) | 3.8 (0.3) | 0.8 (0.3) |
| SS18 | 1659.5 (165.9) | 193.3 (19.3) | 4.5 (0.8) | – | 4.3 (2.5) | – | 1.7 (0.1) | – | 3.7 (0.3) | 2.9 (0.2) | 0.8 (0.3) |
| SS19 | 1534.2 (153.4) | 168.3 (16.8) | 3.3 (0.5) | 0.5 (0.1) | 3.1 (1.1) | – | 1.6 (0.1) | – | 2.3 (0.2) | 1.9 (0.2) | 0.3 (0.1) |
| SS20 | 1683.6 (168.3) | 205.4 (20.5) | 4.3 (0.7) | 0.4 (0.1) | 4.2 (1.6) | – | 2.6 (0.1) | – | 4.4 (0.3) | 4.6 (0.4) | 0.7 (0.1) |
| SS21 | 1430.2 (143.0) | 209.2 (20.9) | 4.0 (0.8) | – | 4.0 (1.7) | – | 2.1 (0.1) | – | 4.0 (0.3) | 4.1 (0.5) | 0.9 (0.2) |
| SB4 | 1713.4 (171.3) | 117.8 (11.7) | 5.7 (0.9) | 3.0 (0.2) | 6.0 (1.5) | 3.2 (0.2) | 2.1 (0.2) | 14.5 (0.1) | 1.8 (0.1) | 1.3 (0.1) | 0.4 (0.1) |
| SS22 | 1272.4 (127.2) | 304.3 (30.4) | 6.2 (0.8) | – | 7.0 (1.7) | – | 3.0 (0.2) | – | 6.5 (0.6) | 5.4 (0.6) | 0.8 (0.1) |
| SS23 | 1371.5 (137.1) | 271.1 (27.1) | 6.4 (0.6) | 0.2 (0.1) | 6.6 (1.0) | – | 3.1 (0.2) | 1.9 (0.1) | 4.6 (0.3) | 4.1 (0.4) | 0.8 (0.1) |
| SS24 | 1208.5 (120.8) | 321.1 (32.1) | 8.3 (1.0) | 0.4 (0.1) | 8.8 (2.3) | – | 3.4 (0.4) | – | 6.0 (0.5) | 5.7 (0.6) | 0.3 (0.1) |
| SS25 | 1655.2 (165.5) | 237.2 (23.7) | 5.2 (1.4) | – | – | – | 1.3 (0.2) | – | 2.6 (0.3) | 3.9 (0.4) | 0.9 (0.2) |
| SS26 | 962.0 (96.2) | 412.7 (41.2) | 10.5 (1.6) | 0.2 (0.2) | 11.5 (4.0) | – | 5.0 (0.4) | – | 7.7 (0.7) | 6.5 (0.6) | 1.1 (0.1) |
| SS27 | 1596.2 (159.6) | 131.3 (13.1) | 3.2 (0.6) | 0.3 (0.1) | 3.4 (0.9) | – | 1.5 (0.1) | – | 2.5 (0.2) | 1.9 (0.2) | 0.5 (0.1) |
| SP1 | 1336.1 (133.6) | 391.4 (39.1) | 9.3 (3.7) | – | – | 8.4 (0.2) | – | – | 8.3 (0.6) | 5.9 (1.5) | – |
| SP2 | 1472.2 (147.2) | 226.8 (22.6) | 5.3 (1.1) | – | 5.8 (5.0) | – | 1.8 (0.5) | – | 3.5 (0.3) | 3.2 (0.3) | 0.5 (0.5) |
| SP3 | 2540.4 (254.1) | 201.9 (20.1) | – | – | – | – | – | – | – | – | 4.7 (2.2) |

[A]The uncertainties in parentheses were calculated in quadrature from those associated with the trace gas emission ratios and *a* ± 10% uncertainty in the assumed fuel carbon across the site, in accordance with (Paton-Walsh *et al.* 2014; Smith *et al.* 2018).
[B]EI, ember ignition; SS, smouldering spread; SB, slash-and-burn; SP, suppression.

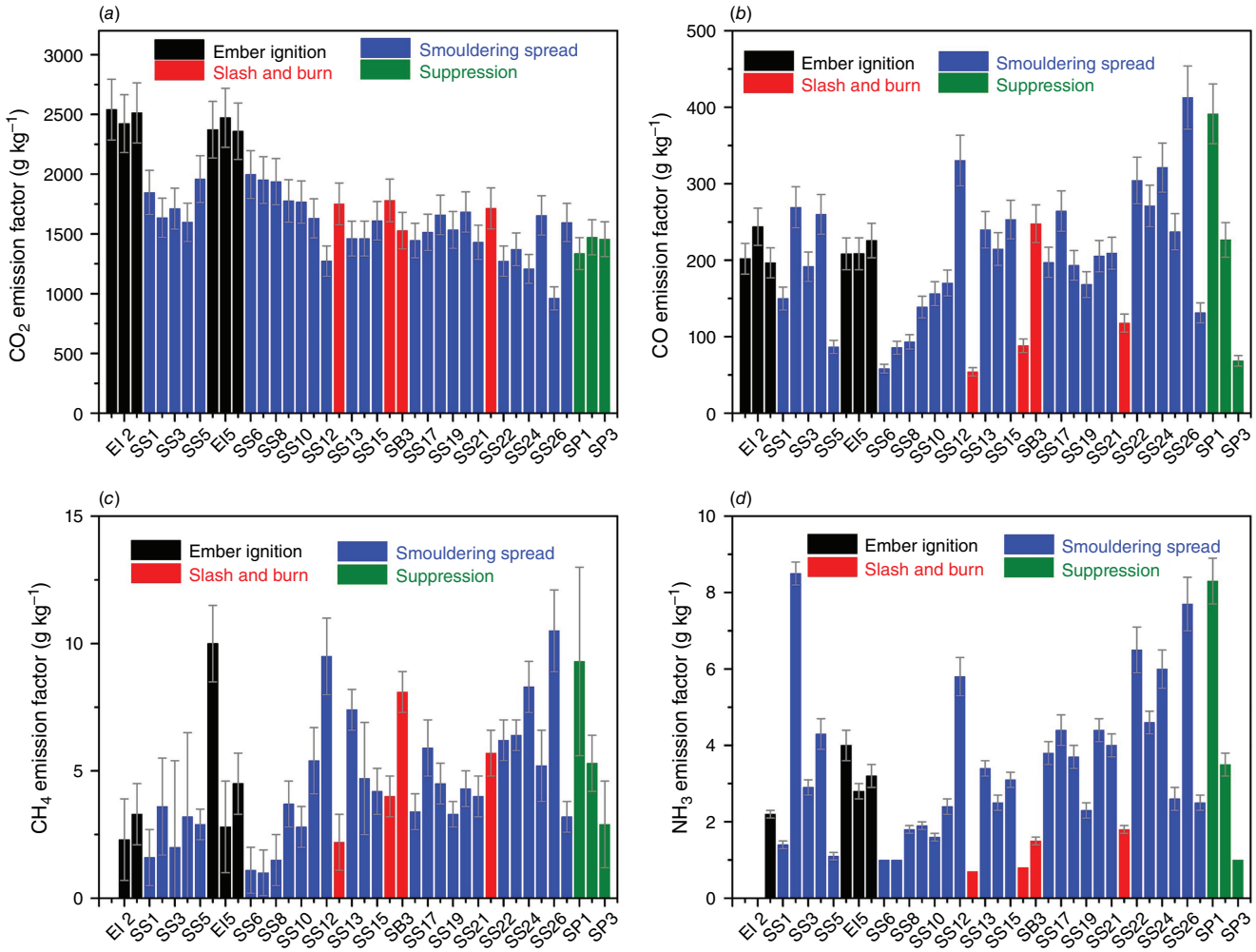


**Fig. 8.** Path-averaged emission factor of $CO_2$ (*a*), CO (*b*), $CH_4$ (*c*), and $NH_3$ (*d*) for all 40 smoke plume measurements.

Independent sample *t*-tests were conducted in this study to statistically examine whether EFs of the four most prominent gas species ($CO_2$, CO, $CH_4$, $NH_3$) from either ember ignition, slash-and-burn, smouldering spread and suppression are significantly different from the others. Specifically, six *t*-tests (two-tailed) with a significance level of 0.05 ($a = 0.05$) were carried out for: (1) ember ignition vs slash-and-burn; (2) ember ignition vs smouldering spread; (3) ember ignition vs suppression; (4) slash-and-burn vs smouldering spread; (5) slash-and-burn vs suppression; and (6) smouldering spread vs suppression (Table 5).

$CO_2$ showed a significantly different EFs ($P < 0.001$) from ember ignition ($n = 6$) than from slash-and-burn ($n = 4$), or smouldering spread ($n = 27$), or suppression ($n = 3$). $CO_2$ EFs from suppression also showed significantly different values than those from slash-and-burn ($P < 0.001$), and from smouldering spread ($P = 0.0077$). However, $CO_2$ failed to differ EFs between slash-and-burn, and smouldering spread ($P = 0.262$). Compared with $CO_2$, CO only performed well in distinguishing ember ignition ($n = 6$) from slash-and-burn ($n = 4$) with $P = 0.0385$. $CH_4$ failed to differ any fire types or fire stages with all *P*-values staying above 0.05. For $NH_3$, a potential gas signature for smouldering peat proposed in (Hu *et al.* 2018*b*), performed well in distinguishing ember ignition ($n = 4$) from slash-and-burn ($n = 4$), and smouldering spread ($n = 27$) from slash-and-burn, with both *P*-values $<0.0001$. More field fire emission measurements are needed for improving the statistical performance of single gas species in differentiating fire types and stages.

## Influence of soil properties on smouldering fire emissions

The percentage difference of EFs of $CO_2$, CO, $CH_4$, and $NH_3$ from the 27 smouldering spread smoke plume measurements stayed at 51.8, 86, 90 and 88%, respectively. In laboratory studies, soil properties (e.g. moisture content, inorganic content and bulk density) have been shown to affect the smouldering fire dynamics (Huang *et al.* 2016; Huang and Rein 2017; Christensen *et al.* 2019; Hu *et al.* 2019, 2020). In this

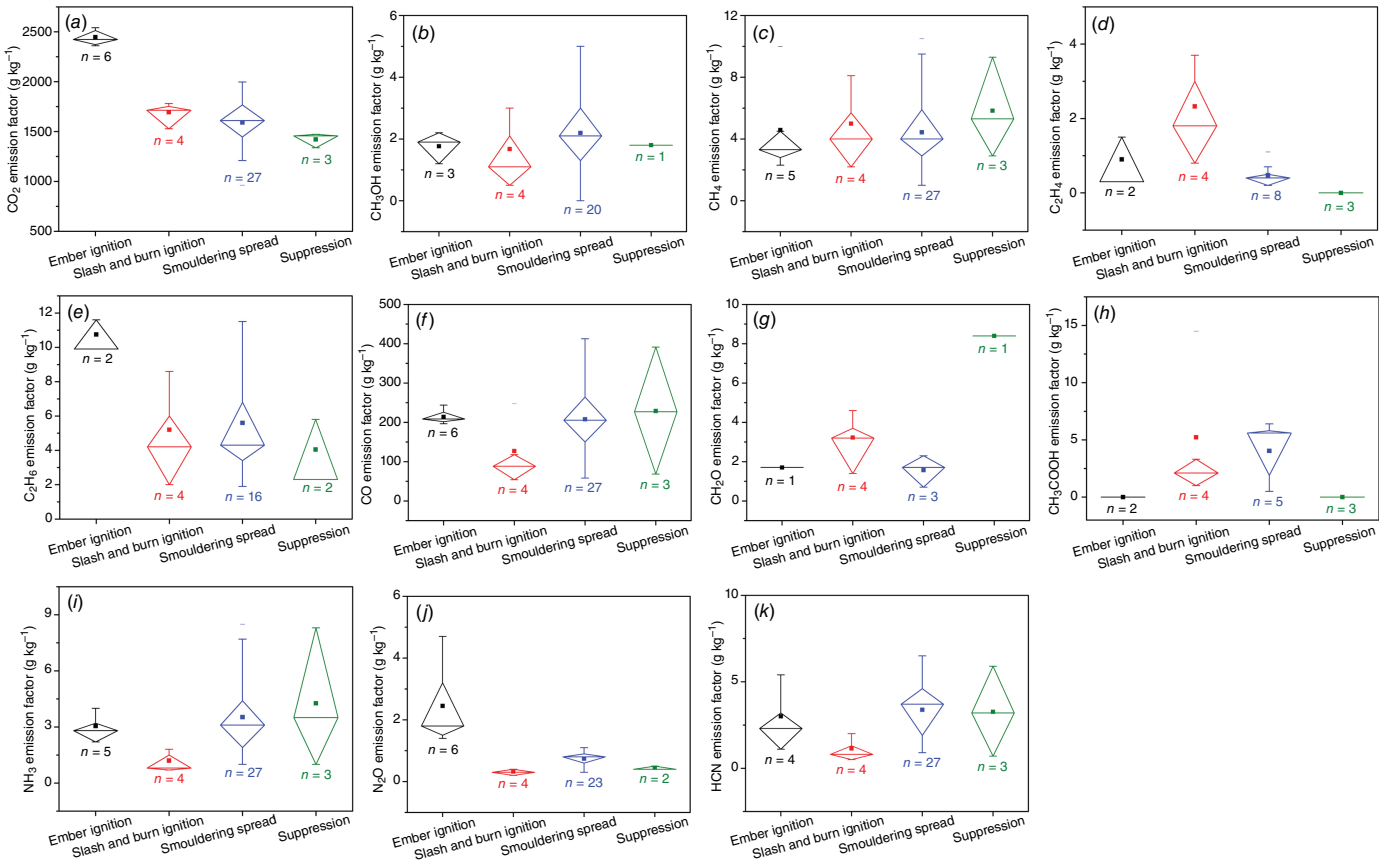


**Fig. 9.** Emission factor of $CO_2$ (*a*), CO (*b*), $CH_4$ (*c*), $C_2H_4$ (*d*), $C_2H_6$ (*e*), $CH_3OH$ (*f*), $CH_2O$ (*g*), $CH_3COOH$ (*h*), $NH_3$ (*i*), $N_2O$ (*j*), and HCN (*k*) from different fire categories. Each box represents groups of emission factor data through their lower quartile (25th percentile), the median (50th percentile) and upper quartile (75th percentile). The mean values are given as solid squares. The error bars show the range of the emission factors in each group.

field experiment, the influence of these soil variables on smouldering fire emissions were examined.

Averaging the soil sampled across depths in the field, peat from P1N was found to have a 225% higher moisture content (173.9 ± 22% in dry basis) than from P1S. Fig. 10 shows the relationships between the peat moisture and the mean EFs of $CO_2$, CO, $CH_4$, and $NH_3$, from plots P1N, P1S, and P2N where fire emissions from the smouldering spread stage were measured. The mean EF of $CO_2$ (1356.5 ± 186.2 g $kg^{-1}$) from smouldering smoke plumes SS13–SS14, SS16, SS21–SS24, and SS26–SS27 measured at P1N were 23% lower than the mean EF value of $CO_2$ from SS1–SS10, SS15, SS17–SS18, and SS20 measured at P1S.

In contrast, the mean EF of CO (225.7 ± 82.5 g $kg^{-1}$) and $CH_4$ (6.0 ± 2.45 g $kg^{-1}$) from P1N was 48.8 and 50.0% higher than the mean EF of CO and $CH_4$ from P1S, respectively. These observed changes in EF with peatland moisture content is in accordance with the findings from laboratory experiments; wet peat has a lower EF of $CO_2$ but a higher EF of CO as moisture content decreases combustion intensities (Hu *et al.* 2019). However, it is worth noting that transient moisture of the peat is susceptible to ambient humidity and rainfall, which vary significantly in the field. More fire emission measurements under diverse moisture conditions are needed to improve the understanding of the influence of moisture on smouldering fire emissions.

Fig. 11 shows the relationships between mean gaseous EFs and the density and inorganic content from P1S, P1N, and P2N. In general, increasing in density leads to a decrease in $CO_2$, but an increase in the EFs of CO, $CH_4$, and $NH_3$. Conversely, when the inorganic content of the peat soil increase, an increase in $CO_2$ and decreases in CO, $CH_4$, and $NH_3$ were observed. Specifically, EFs of $CH_4$ from P1N (6.0 ± 2.5 g $kg^{-1}$) with 72% higher peat bulk density were found to be 99% larger than the EFs of $CH_4$ from P1S. This echoes with the finding from a peat fire emission field study where a strong positive correlation was found between the peat substrate bulk densities with $CH_4$ EFs (Smith *et al.* 2018).

In essence, a higher bulk density can be resulted from either a higher degree of packing, or a higher inorganic content. Higher bulk density fuel with a higher inorganic content may have an improved oxygen supply and thermal conductivity, resulting from the inclusion of smaller and thermally conductive mineral particles in the peat fuel bed. In contrast, higher bulk density peat soils resulting from a tighter structure entails a slower heat loss and a

**Table 4.** Mean emission factors (g kg$^{-1}$, dry basis) and one standard deviation for the whole study and different fire events observed in the field.[A]

| Fire type/stage | $CO_2$ | CO | $CH_4$ | $C_2H_4$ | $C_2H_6$ | $CH_2O$ | $CH_3OH$ | $CH_3COOH$ | $NH_3$ | HCN | $N_2O$ |
|---|---|---|---|---|---|---|---|---|---|---|---|
| Ember ignition ($n$ = 6) | 2446.5 (67.8) | 214.1 (16.0) | 4.5 (2.8) | 0.9 (0.6) | 10.7 (0.8) | 1.7 (0.1) | 1.7 (0.4) | – | 3.0 (0.6) | 3.0 (1.5) | 2.4 (1.1) |
| Slash-and-burn ($n$ = 4) | 1693.3 (98.4) | 127.0 (73.2) | 5.0 (2.1) | 2.3 (1.1) | 5.2 (2.4) | 3.2 (1.1) | 1.6 (0.9) | 5.2 (5.4) | 1.2 (0.4) | 1.1 (0.5) | 0.3 (0.1) |
| Spread ($n$ = 27) | 1590.7 (243.4) | 206.3 (85.0) | 4.3 (2.4) | 0.3 (0.1) | 5.6 (2.6) | 1.2 (0.5) | 2.0 (1.2) | 4.7 (1.9) | 3.5 (2.0) | 3.4 (1.7) | 0.7 (0.2) |
| Suppression ($n$ = 3) | 1421.5 (60.7) | 228.9 (131.8) | 5.8 (2.6) | – | 4.0 (1.7) | 8.4 (0.1) | 1.8 (0.1) | – | 4.2 (3.0) | 3.2 (2.1) | 0.4 (0.1) |
| Study-averaged ($n$ = 40) | 1716 (202) | 202.3 (84.2) | 4.62 (2.47) | 1.06 (1.05) | 5.83 (2.87) | 3.07 (2.20) | 2.03 (1.14) | 4.56 (4.06) | 3.29 (2.03) | 3.09 (1.75) | 0.97 (0.86) |

[A]The values in parentheses were standard deviation of the EFs from the amount of smoke plume measurements ($n$) carried out at each fire category.

limited oxygen supply inside the peat bed, encouraging the formation of incomplete combustion species (e.g. $CH_4$) from peat pyrolysis (Wijedasa *et al.* 2017; Smith *et al.* 2018; Hu *et al.* 2020; Cui 2022). These findings suggest that it is important to map the peatland heterogeneity (e.g. moisture content, inorganic content and bulk density) for a better understanding of spatially variable EFs.

## Influence of field meteorological conditions on smouldering fire emissions

In the field, peatland fires are subjected to wind with varying speeds and directions. In SS11, a burning spot at P1S was partly covered by a metal sheet for 20 min (Table 1). When removing the metal sheet (SS12), the accumulated emissions from the spot was released into the ambient air, resulting in a 27% decrease in $CO_2$ EF but a sharp 111, 239, and 263% increase of EFs for CO, $CH_4$, and $NH_3$, respectively. The field measurement result showed above indicates that changes in oxygen supply and heat loss at smouldering spots could significantly influence fire EFs. Reversely to the metal sheet effect (limited oxygen supply and heat loss from the smouldering spots) demonstrated from SS11 to SS12, strong wind or wind gusts could lead to an enhanced oxygen supply and heat loss at certain smouldering spots *in situ*, potentially introducing inter-plume EF variability (Rein 2016).

Among the 40 smoke plumes measured throughout the experiment, SS19 was conducted during a heavy rain event with an average rain rate of 5.6 mm h$^{-1}$. Compared to SS16 and SS21 (two rain-free measurements at the same location (P1N)), EF of $CO_2$ from SS19 increased 6.7 ± 1.3%, reaching 1534.2 ± 153 g kg$^{-1}$. In contrast, a notable decrease in the values of EFs for CO (−17.2 ± 3.4%), $CH_4$ (−10.8 ± 3.8%), $C_2H_6$ (−25.3 ± 20%), $CH_4O$ (−23.8 ± 2.6%), $NH_3$ (−40.3 ± 6.7%), HCN (−53.7 ± 10.9%), and $N_2O$ (−62.5 ± 36.5%) were found from this SS19 smoke plume influenced by the rain.

Without rainfall, species like $CO_2$ and CO are mainly generated from the oxidation of 'dry char' (Rein *et al.* 2009; Rein 2016). However, the rainfall could convert the 'dry char' into a 'wet char', influencing the composition and concentrations of the fire smoke and thus leading to the changes of the EFs for $CO_2$, CO, $CH_4$, and $C_2H_6$ observed from SS19. The sharp decrease of EFs for gas species like $CH_2O$, $NH_3$, HCN, and $N_2O$ could be partly attributed to the fact that they are soluble in water (rainfall). It is worth noting that the influence of the rain on fire EFs shown here is based on a single rain smoke plume measurement. However, this first investigation of the influence of rainfall on fire emissions opens up opportunities for further study.

Emissions from rain (SS19) and suppression attempts (SP1–SP3) were both influenced by water. Comparing with the EFs from SS19 with rain effect, the averaged EFs from SP1–SP3 measurements presented a mild decrease (7.34%) in the EF value of $CO_2$, but sharp increases in CO (36.0%),

**Table 5.** *T*-test result for comparing emission factors (g kg$^{-1}$, dry basis) between fire events observed in the field.[A]

| | $CO_2$ | | CO | | $CH_4$ | | $NH_3$ | |
|---|---|---|---|---|---|---|---|---|
| | *t*-value | *P*-value | *t*-value | *P*-value | *t*-value | *P*-value | *t*-value | *P*-value |
| EI vs SB | 13.34 | <0.0001 | 2.340 | 0.0385 | 0.253 | 0.8003 | 4.628 | <0.0001 |
| EI vs SS | 15.56 | <0.0001 | 0.44 | 0.6595 | 0.204 | 0.8386 | 1.023 | 0.6125 |
| EI vs SP | 22.9 | <0.0001 | 0.19 | 0.8469 | 0.635 | 0.5253 | 0.684 | 0.9882 |
| SB vs SS | 1.51 | 0.2620 | 1.98 | 0.0960 | 0.585 | 0.5585 | 5.209 | <0.0001 |
| SB vs SP | 4.5 | <0.0001 | 1.20 | 0.4550 | 0.443 | 0.6576 | 1.739 | 0.1642 |
| SS vs SP | 2.89 | 0.0077 | 0.29 | 0.7724 | 0.955 | 0.6788 | 0.3889 | 0.6973 |

[A]EI, ember ignition; SS, smouldering spread; SB, slash-and-burn; SP, suppression.

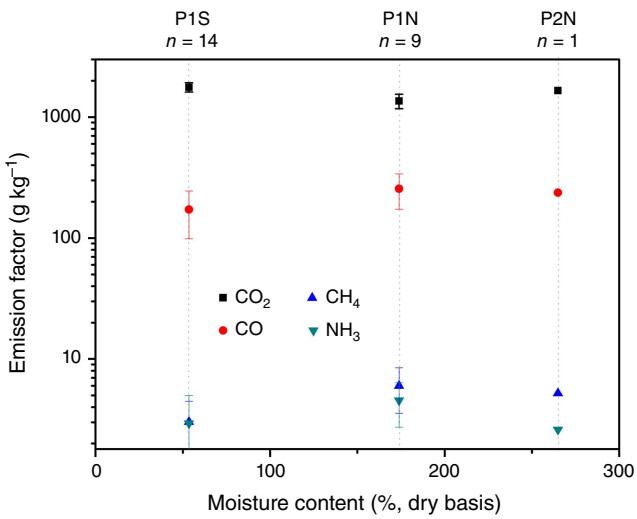


**Fig. 10.** Relationships between the emission factor of $CO_2$, CO, $CH_4$, and $NH_3$ and mean moisture content of the plots P1S, P1N and P2N where fire emissions from smouldering spread were measured. Smoke plumes influenced by limited oxygen supply (SS11–SS12), and rainfall (SS19) were excluded from the results. Only one measurement of smouldering spread fire emissions was carried out in P2N, the data was included in this figure for comparison.

$CH_4$ (75.8%), $C_2H_6$ (29.0%), $NH_3$ (82.6%), and HCN (68.4%). However, owing to the limited measurements for rain ($n$ = 1) and suppression smoke plumes ($n$ = 3), the accurate roles of diverse forms of water (rain, water spay and water injection) in influencing peat fire emissions remain unclear. Further investigations are needed to reveal the mechanisms leading to diverse EFs influenced by different forms and intensities of water. However, this work presents the first field measurements of peat fire EFs during rainfall/suppression, contributing important primary baseline data.

## Modified combustion efficiency (MCE) and fire regimes

In this work, the plume-averaged MCE from all measurements were classified and compared to the fire categories observed during the experiment (Fig. 12). It was found that MCE failed to differentiate the four fire categories that differ fundamentally in terms of the combustion dynamics. For example, the plume-averaged MCE from ember ignition (0.88 ± 0.01) exceeded the 'smouldering MCE range' (between 0.75 and 0.84, or between 0.65 and 0.85) defined in the literature (Akagi *et al.* 2011; Stockwell *et al.* 2016). However, only smouldering combustion was observed throughout the ember ignition attempts. In addition, slash-and-burn, a fire type dominated by flaming combustion, presents a plume-averaged MCE of 0.89 ± 0.06, staying roughly at the same MCE level with smouldering ember ignition.

In the literature, an MCE of 0.9 suggests roughly equal amounts of flaming and smouldering (Akagi *et al.* 2011). However, the plume-averaged MCE for SB4, a plume measurement that mixed partial flaming and smouldering smoke, stayed at 0.8, a typical MCE value for pure smouldering (Akagi *et al.* 2011). The maximum MCE (0.956) found in a smouldering smoke plume (SS6) stayed closely to the 'pure flaming MCE' (0.99) defined in (Stockwell *et al.* 2016). In addition, individual MCE from the three suppression smoke plumes ranged from 0.71 (SP1) to 0.93 (SP3), spanning over the whole literature MCE range for smouldering (Akagi *et al.* 2011; Stockwell *et al.* 2016). Given the large range of the MCE throughout the experiment (0.66–0.96) and the large contradictions seen between the 'MCE-indicated fire regimes' and real fire regimes observed in the field, we conclude that the value of MCE is highly sensitive to complex field variables including fuel heterogeneity and weather conditions (Hu *et al.* 2018*a*).

In a wildfire event, various biomass fuel (e.g. peat and surface vegetation) undergo chemical decomposition by heating from ignition sources (e.g. slash-and-burn, natural lightning or arson), generating gaseous (pyrolysate) and solid (char) products (Rein 2013). Fundamentally, the dominant mode of a fire regime (smouldering or flaming) is dictated when chemical species is oxidised; if the oxidation takes place in the char, smouldering dominants, while if the oxidation happens in the gas phase pyrolysate then flaming combustion dominates (Rein 2016).

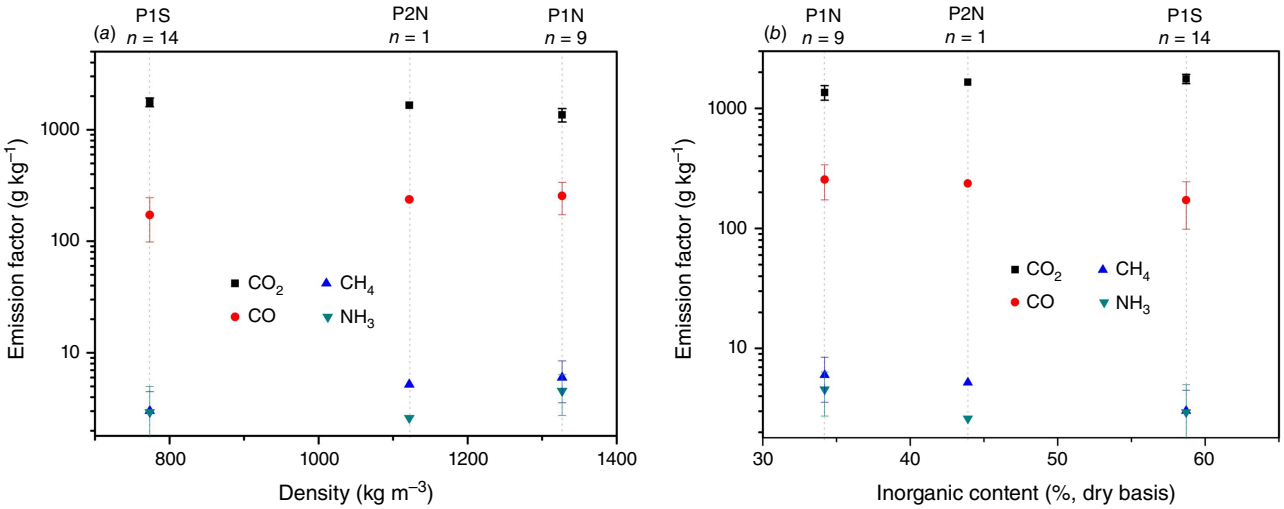


**Fig. 11.** Relationships between the emission factor of $CO_2$, CO, $CH_4$, and $NH_3$ and mean density (*a*) and inorganic contents (*b*) of the plots P1S, P1N, and P2N where fire emissions from smouldering spread were measured. Smoke plumes influenced by limited oxygen supply (SS11–SS12), and rainfall (SS19) were excluded from the results. Only one measurement of smouldering spread fire emissions was carried out in P2N, the data was included in this figure for comparison.

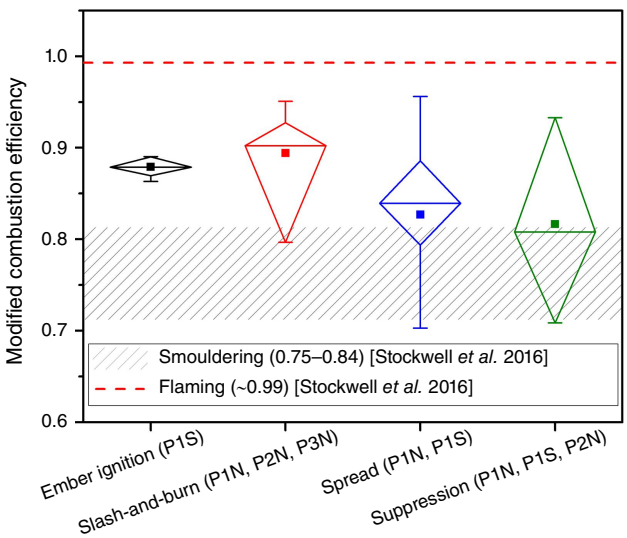


**Fig. 12.** Plume-averaged modified combustion efficiency from the smoke measurements of ember ignition, slash-and-burn, smouldering, and suppression. Each box represents groups of data through their lower quartile (25th percentile), the median (50th percentile), upper quartile (75th percentile). The mean values are given as solid squares. The error bars show the range of the modified combustion efficiency in each group.

In this experiment, fire emissions are affected by the peatland heterogeneity and complex weather conditions. These field ('real world') variables could have substantial influence on the transient $CO_2$ and CO emissions and in turn, lead to significant variations of the associated values of MCE (see Fig. S3 for the transient $CO_2$, CO, and MCE for SS26 as an example). MCE greatly simplifies the complex fire dynamics that drive changes in fire emissions, and fails to incorporate the fundamental difference between flaming and smouldering combustion (Hu *et al.* 2018*b*). As a result, large uncertainties could be introduced when using a single MCE value to determine the regimes of a wildland fire.

It is worth noting that comparing to natural smouldering peatland fires spreading thousands of $km^2$ and releasing emissions over weeks or even months, the smouldering area of the GAMBUT fire experiment (408 $m^2$), as well as the number of the smoke plume measurements ($n$ = 40) conducted in this research remain limited. Furthermore, uncertainties exist in terms of the accuracy of the EFs and MCE reported from the FTIR measurements of plume emissions subjected to wind gusts and potential mixing of emissions from adjacent burns. However, this field fire research provides a framework for an advanced understanding of temporally variable EFs and emissions inventories from fires on degraded tropical peatlands.

## Conclusions

We conducted the first controlled field-scale tropical peatland fires in Sumatra, Indonesia. 'Life-cycle' fire emission factors (EFs) of 11 gas species from various fire stages, including ignition, spread, and suppression, were characterised and quantified using open-path FTIR spectroscopy from 40 smoke plumes throughout a 12-day field measurement campaign. These represented the first published EFs for fires burning in degraded peatland, which had been subjected to long-term degradation, restoration, or agricultural conversion with distinctively high inorganic content. We found EFs of similar magnitude to those reported in the literature (Akagi *et al.* 2011; Hu *et al.* 2018*a*). Incorporating

mean EFs from different fire categories (Table 4) into fire emission inventories could improve the accuracy of atmospheric modelling and the overall emission estimates for tropical peatland regions with high fire frequency.

Similar to a handful of field studies of tropical peatland fire emissions (Huijnen *et al.* 2016; Stockwell *et al.* 2016; Smith *et al.* 2018), substantial inter-plume variability was found for EFs of different species. We presented the first field evidence suggesting that much of these variability could be determined by fuel types (e.g. charcoal ember vs peat), fire types (flaming vs smouldering), fire stages (ignition vs spread vs suppression), fuel heterogeneity (e.g. moisture content, inorganic content, and bulk density), and field meteorological conditions (e.g. strong wind or rainfall).

Large contradictions were found between the 'MCE-defined fire regimes' and the real fire regimes from *in situ* observations. Thus, we concluded that MCE is highly sensitive to complex field variables and when used alone, can introduce significant uncertainty in determining fire regimes in heterogeneous field environments.

Fundamental understanding of obtained from small-scale laboratory experiments (e.g. Hu *et al.* (2019)) serve well for explaining the variability of EFs and MCE from this GAMBUT peat fire experiment, highlighting the importance of coupling laboratory experiments with field measurements towards a better understanding of peatland fire emissions and reducing the impact of large-scale smouldering wildfires.

## Supplementary material

Supplementary material is available online.

## References


Akagi SK, Yokelson RJ, Wiedinmyer C, Alvarado MJ, Reid JS, Karl T, Crounse JD, Wennberg PO (2011) Emission factors for open and domestic biomass burning for use in atmospheric models. *Atmospheric Chemistry and Physics* **11**, 4039–4072. doi:10.5194/ACP-11-4039-2011

Archibald S, Lehmann CE, Belcher CM, Bond WJ, Bradstock RA, Daniau AL, Dexter KG, Forrestel EJ, Greve M, He T, Higgins SI (2018) Biological and geophysical feedbacks with fire in the Earth system. *Environmental Research Letters* **13**, 033003. doi:10.1088/1748-9326/aa9ead

BMKG (2022) Indonesia online climate database. Available at http://dataonline.bmkg.go.id/data_iklim

Bowman DM, Balch JK, Artaxo P, Bond WJ, Carlson JM, Cochrane MA, D'Antonio CM, DeFries RS, Doyle JC, Harrison SP, Johnston FH, Keeley JE, Krawchuk MA, Kull CA, Marston JB, Moritz MA, Prentice IC, Roos CI, Scott AC, Swetnam TW, van der Werf GR, Pyne SJ (2009) Fire in the Earth system. *Science* **324**, 481–484. doi:10.1126/science.1163886

Christensen EG, Hu Y, Restuccia F, Santoso MA, Rein G (2019) Experimental Methods and Scales in Smouldering Wildfires. In 'Fire effects on soils properties'. (Eds P Pereira, J Mataix-Solera, X Ubeda, G Rein, A Cerda) pp. 267–280. (CSIRO Publishing: Melbourne, Vic, Australia)

Christian TJ, Kleiss B, Yokelson RJ, Holzinger R, Crutzen PJ, Hao WM, Saharjo BH, Ward DE (2003) Comprehensive laboratory measurements of biomass-burning emissions: 1. Emissions from Indonesian, African, and other fuels. *Journal of Geophysical Research* **108**, 4719. doi:10.1029/2003JD003704

Cochrane MA (2003) Fire science for rainforests. *Nature* **421**, 913–919. doi:10.1038/nature01437

Cui W (2022) Laboratory investigation of the ignition and spread of smouldering in peat samples of different origins and the associated emissions. PhD Thesis, Imperial College London, London, UK.

Eggleston HS, Buendia L, Miwa K, Ngara T, Tanabe K (Eds) (2006) '2006 IPCC guidelines for national greenhouse gas inventories. Vol. 5.' (Institute for Global Environmental Strategies: Hayama, Japan)

Forsyth T (2014) Public concerns about transboundary haze: a comparison of Indonesia, Singapore, and Malaysia. *Global Environmental Change* **25**, 76–86. doi:10.1016/j.gloenvcha.2014.01.013

Gordon IE, Rothman LS, Hill C, Kochanov RV, Tan Y, Bernath PF, Birk M, Boudon V, Campargue A, Chance KV, Drouin BJ (2017) The HITRAN2016 molecular spectroscopic database. *Journal of Quantitative Spectroscopy and Radiative Transfer* **203**, 3–69. doi:10.1016/j.jqsrt.2017.06.038

Griffith DW (1996) Synthetic calibration and quantitative analysis of gas-phase FT-IR spectra. *Applied Spectroscopy* **50**, 59–70.

Heil A, Goldammer J (2001) Smoke-haze pollution: a review of the 1997 episode in Southeast Asia. *Regional Environmental Change* **2**, 24–37. doi:10.1007/s101130100021

Hiraishi T, Krug T, Tanabe K, Srivastava N, Baasansuren J, Fukuda M, Troxler TG (2014) '2013 supplement to the 2006 IPCC guidelines for national greenhouse gas inventories: Wetlands.' (IPCC: Switzerland)

Hu Y, Fernan De Z-Anez N, Smith T, Rein G (2018*a*) Review of emissions from smouldering peat fires and their contribution to regional haze episodes. *International Journal of Wildland Fire* **27**, 293–312. doi:10.1071/WF17084

Hu Y, Christensen EG, Restuccia F, Rein G (2018*b*) Transient gas and particle emissions from smouldering combustion of peat. *Proceedings of the Combustion Institute* **37**, 4035–4042. doi:10.1016/j.proci.2018.06.008

Hu Y, Christensen EG, Amin HMF, Smith TEL, Rein G (2019) Experimental study of moisture content effects on the transient gas and particle emissions from peat fires. *Combustion and Flame* **209**, 408–417. doi:10.1016/j.combustflame.2019.07.046

Hu Y, Cui W, Rein G (2020) Haze emissions from smouldering peat: the roles of inorganic content and bulk density. *Fire Safety Journal* **113**, 102940. doi:10.1016/j.firesaf.2019.102940

Hu Y, Smith TEL, Santoso MA, Amin HMF, Christensen E, Cui W, Purnomo DMJ, Nugroho YS, Rein G (2024) GAMBUT field measurement of emissions from a tropical peatland fire experiment: from ignition to spread to suppression (Version 1.0.0). [Dataset] Zenodo.

Huang X, Rein G (2017) Downward spread of smouldering peat fire: the role of moisture, density and oxygen supply. *International Journal of Wildland Fire* **26**, 907–918. doi:10.1071/WF16198

Huang RJ, Zhang Y, Bozzetti C, Ho KF, Cao JJ, Han Y, Daellenbach KR, Slowik JG, Platt SM, Canonaco F, Zotter P, Wolf R, Pieber SM, Bruns EA, Crippa M, Ciarelli G, Piazzalunga A, Schwikowski M, Abbaszade G, Schnelle-Kreis J, Zimmermann R, An Z, Szidat S, Baltensperger U, El Haddad I, Prévôt AS (2014) High secondary aerosol contribution to particulate pollution during haze events in China. *Nature* **514**, 218–222. doi:10.1038/nature13774

Huang X, Restuccia F, Gramola M, Rein G (2016) Experimental study of the formation and collapse of an overhang in the lateral spread of smouldering peat fires. *Combustion and Flame* **168**, 393–402. doi:10.1016/j.combustflame.2016.01.017

Huijnen V, Wooster MJ, Kaiser JW, Gaveau DLA, Flemming J, Parrington M, Inness A, Murdiyarso D, Main B, van Weele M (2016) Fire carbon emissions over maritime south-east Asia in 2015 largest since 1997. *Scientific Reports* **6**, 26886. doi:10.1038/SREP26886

Jauhiainen J, Page SE, Vasander H (2016) Greenhouse gas dynamics in degraded and restored tropical peatlands. *Mires and Peat* **17**, 1–12. doi:10.19189/MaP.2016.OMB.229

Kettridge N, Turetsky MR, Sherwood JH, Thompson DK, Miller CA, Benscoter BW, Flannigan MD, Wotton BM, Waddington JM (2015) Moderate drop in water table increases peatland vulnerability to post-fire regime shift. *Scientific Reports* **5**, 8063. doi:10.1038/SREP08063

Koplitz SN, Mickley LJ, Marlier ME, Buonocore JJ, Kim PS, Liu T, Sulprizio MP, DeFries RS, Jacob DJ, Schwartz J, Pongsiri M (2016) Public health impacts of the severe haze in Equatorial Asia in September–October 2015: demonstration of a new framework for

informing fire management strategies to reduce downwind smoke exposure. *Environmental Research Letters* **11**, 094023. doi:10.1088/1748-9326/11/9/094023

Kunii O, Kanagawa S, Yajima I, Hisamatsu Y, Yamamura S, Amagai T, Ismail IT (2002) The 1997 haze disaster in Indonesia: its air quality and health effects. *Archives of Environmental Health* **57**, 16–22. doi:10.1080/00039890209602912

Matysek M, Evers S, Samuel M K, Sjogersten S (2018) High heterotrophic $CO_2$ emissions from a Malaysian oil palm plantation during dry-season. *Wetlands Ecology Management* **26**, 415–424. doi:10.1007/s11273-017-9583-6

Page SE, Siegert F, Rieley JO, Boehm HD, Jaya A, Limin S (2002) The amount of carbon released from peat and forest fires in Indonesia during 1997. *Nature* **420**, 61–65. doi:10.1038/NATURE01131

Page SE, Rieley JO, Banks CJ (2011) Global and regional importance of the tropical peatland carbon pool. *Global Change Biology* **17**, 798–818. doi:10.1111/j.1365-2486.2010.02279.x

Pastor E, Oliveras I, Urquiaga-Flores E, Quintano-Loayza JA, Manta MI, Planas E (2017) A new method for performing smouldering combustion field experiments in peatlands and rich-organic soils. *International Journal of Wildland Fire* **26**, 1040–1052. doi:10.1071/WF17033

Paton-Walsh C, Smith TE, Young EL, Griffith DW, Guérette ÉA (2014) New emission factors for Australian vegetation fires measured using open-path Fourier transform infrared spectroscopy–Part 1: Methods and Australian temperate forest fires. *Atmospheric Chemistry and Physics* **14**, 11313–11333. doi:10.5194/acp-14-11313-2014

Plautz J (2018) Piercing the haze. *Science* **361**, 1060–1063. doi:10.1126/science.361.6407.1060

Rein G (2013) Smouldering fires and natural fuels. In 'Fire phenomena and the Earth system: an interdisciplinary guide to fire science'. (Ed. CM Belcher) pp. 15–34. (John Wiley & Sons: Oxford, UK)

Rein G (2016) Smouldering combustion. In 'The SFPE handbook of fire protection engineering'. (Ed. MJ Hurley) pp. 581–603. (Springer: New York, NY, USA)

Rein G, Cleaver N, Ashton C, Pironi P, Torero JL (2008) The severity of smouldering peat fires and damage to the forest soil. *Catena* **74**, 304–309. doi:10.1016/j.catena.2008.05.008

Rein G, Cohen S, Simeoni A (2009) Carbon emissions from smouldering peat in shallow and strong fronts. *Proceedings of the Combustion Institute* **32**, 2489–2496. doi:10.1016/J.PROCI.2008.07.008

Restuccia F, Huang X, Rein G (2017) Self-ignition of natural fuels: can wildfires of carbon-rich soil start by self-heating? *Fire Safety Journal* **91**, 828–834. doi:10.1016/j.firesaf.2017.03.052

Santoso MA, Christensen EG, Amin HM, Palamba P, Hu Y, Purnomo DM, Cui W, Pamitran A, Richter F, Smith TE, Nugroho YS (2022) GAMBUT field experiment of peatland wildfires in Sumatra: from ignition to spread and suppression. *International Journal of Wildland Fire* **31**, 949–966. doi:10.1071/WF21135

Shaposhnikov D, Revich B, Bellander T, Bedada GB, Bottai M, Kharkova T, Kvasha E, Lezina E, Lind T, Semutnikova E, Pershagen G (2014) Mortality related to air pollution with the Moscow heat wave and wildfire of 2010. *Epidemiology* **25**, 359–364. doi:10.1097/EDE.0000000000000090

Smith TE, Wooster MJ, Tattaris M, Griffith DW (2011) Absolute accuracy and sensitivity analysis of OP-FTIR retrievals of $CO_2$, $CH_4$ and CO over concentrations representative of "clean air" and "polluted plumes". *Atmospheric Measurement Techniques* **4**, 97–116. doi:10.5194/amt-4-97-2011

Smith TE, Paton-Walsh C, Meyer CP, Cook GD, Maier SW, Russell-Smith J, Wooster MJ, Yates CP (2014) New emission factors for Australian vegetation fires measured using open-path Fourier transform infrared spectroscopy–Part 2: Australian tropical savanna fires. *Atmospheric Chemistry and Physics* **14**, 11335–11352. doi:10.5194/acp-14-11335-2014

Smith TEL, Evers S, Yule CM, Gan JY (2018) In situ tropical peatland fire emission factors and their variability, as determined by field measurements in Peninsula Malaysia. *Global Biogeochemical Cycles* **32**, 18–31. doi:10.1002/2017GB005709

Stockwell CE, Yokelson RJ, Kreidenweis SM, Robinson AL, DeMott PJ, Sullivan RC, Reardon J, Ryan KC, Griffith DW, Stevens L (2014) Trace gas emissions from combustion of peat, crop residue, domestic biofuels, grasses, and other fuels: Configuration and Fourier-transform infrared (FTIR) component of the fourth Fire Lab at Missoula Experiment (FLAME-4). *Atmospheric Chemistry and Physics* **14**, 9727–9754. doi:10.5194/ACP-14-9727-2014

Stockwell CE, Jayarathne T, Cochrane MA, Ryan KC, Putra EI, Saharjo BH, Nurhayati AD, Albar I, Blake DR, Simpson IJ, Stone EA (2016) Field measurements of trace gases and aerosols emitted by peat fires in central Kalimantan, Indonesia, during the 2015 El Nino. *Atmospheric Chemistry and Physics* **16**, 11711–11732. doi:10.5194/ACP-16-11711-2016

Turetsky MR, Benscoter B, Page S, Rein G, van der Werf GR, Watts A (2015) Global vulnerability of peatlands to fire and carbon loss. *Nature Geoscience* **8**, 11–14. doi:10.1038/NGEO2325

Urbanski S (2014) Wildland fire emissions, carbon, and climate: emission factors. *Forest Ecology and Management* **317**, 51–60. doi:10.1016/j.foreco.2013.05.045

Usup A, Hashimoto Y, Takahashi H, Hayasaka H (2004) Combustion and thermal characteristics of peat fire in tropical peatland in Central Kalimantan, Indonesia. *Tropics* **14**, 1–19. doi:10.3759/tropics.14.1

van der Werf GR, Randerson JT, Giglio L, Van Leeuwen TT, Chen Y, Rogers BM, Mu M, Van Marle MJ, Morton DC, Collatz GJ, Yokelson RJ (2017) Global fire emissions estimates during 1997–2016. *Earth System Science Data* **9**, 697–720. doi:10.5194/essd-9-697-2017

van Leeuwen TT, van der Werf GR (2011) Spatial and temporal variability in the ratio of trace gases emitted from biomass burning. *Atmospheric Chemistry and Physics* **11**, 3611–3629. doi:10.5194/acp-11-3611-2011

Ward DE, Hao W (1991) Projections of emissions from burning of biomass foruse in studies of global climate and atmospheric chemistry. In 'Paper 91-128.4. Presented at the 84th Annual Meeting and Exhibition', 16–21 June 1991. 16 p. (Air and Waste Management Association: Vancouver, BC, Canada)

Ward DE, Radke LF (1993) Emissions measurements from vegetation fires: a comparative evaluation of methods and results. In 'Fire in the environment: the ecological, atmospheric, and climatic importance of vegetation fires'. (Eds PJ Crutzen, JG Goldammer) pp. 53–76. (John Wiley & Sons: Oxford, UK)

Wiggins EB, Czimczik CI, Santos GM, Chen Y, Xu X, Holden SR, Randerson JT, Harvey CF, Kai FM, Yu LE (2018) Smoke radiocarbon measurements from Indonesian fires provide evidence for burning of millennia-aged peat. *Proceedings of the National Academy of Sciences of the United States of America* **115**, 12419–12424. doi:10.1073/pnas.1806003115

Wijedasa LS, Jauhiainen J, Könönen M, Lampela M, Vasander H, Leblanc MC, Evers S, Smith TE, Yule CM, Varkkey H, Lupascu M, Parish F, Singleton I, Clements GR, Aziz SA, Harrison ME, Cheyne S, Anshari GZ, Meijaard E, Goldstein JE, Waldron S, Hergoualc'h K, Dommain R, Frolking S, Evans CD, Posa MR, Glaser PH, Suryadiputra N, Lubis R, Santika T, Padfield R, Kurnianto S, Hadisiswoyo P, Lim TW, Page SE, Gauci V, Van Der Meer PJ, Buckland H, Garnier F, Samuel MK, Choo LN, O'Reilly P, Warren M, Suksuwan S, Sumarga E, Jain A, Laurance WF, Couwenberg J, Joosten H, Vernimmen R, Hooijer A, Malins C, Cochrane MA, Perumal B, Siegert F, Peh KS, Comeau LP, Verchot L, Harvey CF, Cobb A, Jaafar Z, Wösten H, Manuri S, Müller M, Giesen W, Phelps J, Yong DL, Silvius M, Wedeux BM, Hoyt A, Osaki M, Hirano T, Takahashi H, Kohyama TS, Haraguchi A, Nugroho NP, Coomes DA, Quoi LP, Dohong A, Gunawan H, Gaveau DL, Langner A, Lim FK, Edwards DP, Giam X, Van Der Werf G, Carmenta R, Verwer CC, Gibson L, Gandois L, Graham LL, Regalino J, Wich SA, Rieley J, Kettridge N, Brown C, Pirard R, Moore S, Capilla BR, Ballhorn U, Ho HC, Hoscilo A, Lohberger S, Evans TA, Yulianti N, Blackham G, Onrizal , Husson S, Murdiyarso D, Pangala S, Cole LE, Tacconi L, Segah H, Tonoto P, Lee JS, Schmilewski G, Wulffraat S, Putra EI, Cattau ME, Clymo RS, Morrison R, Mujahid A, Miettinen J, Liew SC, Valpola S, Wilson D, D'Arcy L, Gerding M, Sundari S, Thornton SA, Kalisz B, Chapman SJ, Su AS, Basuki I, Itoh M, Traeholt C, Sloan S, Sayok AK, Andersen R (2017) Denial of long-term issues with agriculture on tropical peatlands will have devastating consequences. *Global Change Biology* **23**, 977–982. doi:10.1111/gcb.13516

Wilson D, Dixon SD, Artz RR, Smith TE, Evans CD, Owen HJ, Archer E, Renou-Wilson F (2015) Deviation of greenhouse gas emission factors for peatlands managed for extraction in the Republic of Ireland and the United Kingdom. *Biogeosciences* **12**, 5291–5308. doi:10.5194/BG-12-5291-2015

Wooster MJ, Freeborn PH, Archibald S, Oppenheimer C, Roberts GJ, Smith TE, Govender N, Burton M, Palumbo I (2011) Field determination of biomass burning emission ratios and factors via open-path FTIR spectroscopy and fire radiative power assessment: headfire, backfire and residual smouldering combustion in African savannahs. *Atmospheric Chemistry and Physics* **11**, 11591–11615. doi:10.5194/acp-11-11591-2011

Yokelson RJ, Griffith DW, Ward DE (1996) Open-path Fourier transform infrared studies of large-scale laboratory biomass fires. *Journal of Geophysical Research: Atmospheres* **101**, 21067–21080. doi:10.1029/96JD01800

Yokelson RJ, Susott R, Ward DE, Reardon J, Griffith DW (1997) Emissions from smoldering combustion of biomass measured by open-path Fourier transform infrared spectroscopy. *Journal of Geophysical Research, D, Atmospheres* **102**, 18865–18877. doi:10.1029/97JD00852

Yokelson RJ, Karl T, Artaxo P, Blake DR, Christian TJ, Griffith DW, Guenther A, Hao WM (2007) The Tropical Forest and Fire Emissions Experiment: overview and airborne fire emission factor measurements. *Atmospheric Chemistry and Physics* **7**, 5175–5196. doi:10.5194/acp-7-5175-2007

**Data availability.** Data are available in the paper by Hu *et al.* (2024).

**Conflicts of interest.** The authors declare no conflicts of interest.

**Declaration of funding.** This study was funded by the National Natural Science Foundation of China (52106184), The European Research Council Consolidator Grant Haze (682587), the Natural Science Foundation of Sichuan Province (2023NSFSC0189), Sichuan Fire Research Institution Basic Research Funds (Z20238801, Z202488111Z), the Engineering and Physical Sciences Research Council Global Challenges Research Fund GAMBUT (United Kingdom) and Ministry of Research, Technology, and Higher Education of the Republic of Indonesia and Universitas Indonesia Penelitian Terapan Unggulan Perguruan Tinggi 2018 (514/UN2.R3.1/HKP05.00/2018); Lembaga Pengelola Dana Pendidikan Indonesia Doctorate Scholarship (Republic of Indonesia); Ministry of Internal Affairs of the Republic of Indonesia; and The Natural Environment Research Council Field Spectroscopy Facility (United Kingdom).

**Acknowledgements.** We thank the many collaborators and colleagues who provided vital support to GAMBUT along the way. We particularly thank the team in the field from Universitas Indonesia (Mad Yasin and Hafizha Mulyasih), Balai Diklat Satpol PP dan Damkar Rokan Hilir (Setyawan, Chairullah, Chandra Dorman Lolle, Dedi Hariyanto, Iskandar, Parison, and Rizal), Universitas Riau (Ari Sandhyavitri, Awaluddin Martin, Harun Orion Purba, Yogi Wibowo Agusta, Rizki Ramadhan Husaini, Guspi, Muhamad Yusa, and Doni, Jamal), and local workers in Rokan Hilir (Adnan and team, and Herman). We thank the team that remotely assisted from Imperial College London (Francesco Restuccia, Franz Richter, Guoxiang Zhao, Han Yuan, Xuanze He, and Nieves Fernandez Anes) and Universitas Indonesia in Depok (Jefri Alfonso Sigalingging, Nadhira Gilang Ratnasari, Aditya Hartawan, and Hanifa Khansa Zhafira). We are grateful for the discussions and advice from Rizari (Ministry of Internal Affairs of the Republic of Indonesia), Evan Nur Setya Hadi (Ministry of Internal Affairs of the Republic of Indonesia), Bambang Hero (Institut Pertanian Bogor), and Haris Gunawan (Peatland Restoration Agency).

**Author affiliations**

[A]Department of Mechanical Engineering, Imperial College London, London, SW7 2AZ, UK.

[B]Sichuan Fire Research Institution, Ministry of Emergency Management of China, Chengdu, 610036, China.

[C]Department of Geography and Environment, London School of Economics and Political Science, London, WC2A 2AE, UK.

[D]Department of Mechanical Engineering, Faculty of Engineering, Universitas Indonesia, Depok, 16424, Indonesia.

[E]School of Computing, Engineering & Digital Technologies, Teesside University, Middlesbrough, TS1 3BA, UK.